

PUBLIC ROADS

A JOURNAL OF HIGHWAY RESEARCH



UNITED STATES DEPARTMENT OF AGRICULTURE
BUREAU OF PUBLIC ROADS



VOL. 8, NO. 3



MAY, 1927



GRAVEL ROAD AT ARLINGTON EXPERIMENTAL STATION

PUBLIC ROADS

A JOURNAL OF HIGHWAY RESEARCH

U. S. DEPARTMENT OF AGRICULTURE

BUREAU OF PUBLIC ROADS

CERTIFICATE: By direction of the Secretary of Agriculture, the matter contained herein is published as administrative information and is required for the proper transaction of the public business

VOL. 8, NO. 3

MAY, 1927

R. E. ROYALL, Editor

TABLE OF CONTENTS

	Page
Principles of Final Soil Classification	41
Analysis of Stresses in Concrete Roads Caused by Variations of Temperature	54

THE U. S. BUREAU OF PUBLIC ROADS

Willard Building, Washington, D. C.

REGIONAL HEADQUARTERS

Mark Sheldon Building, San Francisco, Calif.

DISTRICT OFFICES

DISTRICT No. 1, Oregon, Washington, and Montana.
Box 3900, Portland, Oreg.

DISTRICT No. 2, California, Arizona, and Nevada.
Mark Sheldon Building, San Francisco, Calif.

DISTRICT No. 3, Colorado, New Mexico, and Wyoming.
301 Customhouse Building, Denver, Colo.

DISTRICT No. 4, Minnesota, North Dakota, South Dakota, and Wisconsin.
410 Hamm Building, St. Paul, Minn.

DISTRICT No. 5, Iowa, Kansas, Missouri, and Nebraska.
8th Floor, Saunders-Kennedy Building, Omaha, Nebr.

DISTRICT No. 6, Arkansas, Oklahoma, and Texas.
1912 F. & M. Bank Building, Fort Worth, Tex.

DISTRICT No. 7, Illinois, Indiana, Kentucky, and Michigan.
South Chicago Post Office Building, Chicago, Ill.

DISTRICT No. 8, Alabama, Louisiana, Georgia, Florida, Mississippi, South Carolina, and Tennessee.
Box J, Montgomery, Ala.

DISTRICT No. 9, Connecticut, Maine, Massachusetts, New Hampshire, New Jersey, New York, Rhode Island, and Vermont.
Federal Building, Troy, N. Y.

DISTRICT No. 10, Delaware, Maryland, North Carolina, Ohio, Pennsylvania, Virginia, and West Virginia.
Willard Building, Washington, D. C.

DISTRICT No. 11, Alaska.
Goldstein Building, Juneau, Alaska.

DISTRICT No. 12, Idaho and Utah.
Fred J. Kiesel Building, Ogden, Utah.

Owing to the necessarily limited edition of this publication it will be impossible to distribute it free to any persons or institutions other than State and county officials actually engaged in planning or constructing public highways, instructors in highway engineering, periodicals upon an exchange basis, and Members of both Houses of Congress. Others desiring to obtain "Public Roads" can do so by sending 10 cents for a single number or \$1 per year to the Superintendent of Documents, Government Printing Office, Washington, D. C.

PRINCIPLES OF FINAL SOIL CLASSIFICATION

By Dr. CHARLES TERZAGHI, Massachusetts Institute of Technology, Research Consultant to the Bureau of Public Roads

IF THE foundations of a building settle excessively, thus causing cracking of the walls and ceilings, the reason thereof may reside in excessive compressibility of the soil or lateral flow of the material or both of these factors combined. The speed with which the soil is compressed by the load depends on the permeability of the soil. The more permeable the soil the more rapidly the excess water can escape. Hence, if we wish to describe the properties of a soil, its compressibility and its permeability must be determined and these properties expressed in standard terms.

Cracking of a road surface caused by subsurface conditions may be due to excessive compressibility of the subgrade, to lateral squeezing out of the subgrade, to excessive volume change associated with swelling after a period of drought, to slaking of the material in the shoulders of the road, or to expansion caused by freezing. If the soil is both compressible and permeable the cracking will result essentially from compression of the material caused by pressure. If it is compressible but at the same time very feebly permeable, the failure will be due to lateral flow. The intensity of swelling is simply determined by the degree of elasticity of the material. The slaking properties of the soil depend on both the modulus of swelling and on the permeability. Hence, if we wish to describe the properties of the subgrade of a road which has failed, we have to investigate the factors which influence the amount and the speed of compression of the subgrade under pressure and the volume change due to drying and wetting. These are the outstanding factors in the proposed system of final soil classification. We want to describe our soils not by more or less abstract figures like the Atterberg limits, the dye adsorption number, the moisture equivalent, etc., which are suitable for preliminary purposes only, but rather by data with a direct, simple, and well-known bearing on the behavior of the subgrade.

COMPRESSIBILITY AND ELASTICITY OF SOILS STUDIED

The term "compressibility" refers to the compression produced by a pressure acting on the soil. Suppose we have a layer of fairly loose sand, laterally confined. If the surface of this layer is loaded with 0.5 kilogram per square centimeter (about 0.5 ton per square foot), a measurement of the density of the loaded material may show that the voids occupy a volume equal to 0.97 times the volume occupied by the grains. We say the sand has a voids ratio of 0.97 (ratio between the volume of the voids and the volume occupied by the solids). If the pressure is raised from 0.5 to 3 kilograms per square centimeter, its voids ratio drops from 0.97 to 0.93, which means that the volume of the voids decreases by 4 per cent of the volume occupied by the solids. The voids ratio of a Mississippi clay (fig. 1, A) under a pressure of 0.5 kilogram per square centimeter was found to be equal to 1.67. When the pressure was raised from 0.5 to 3 kilograms per square centimeter the voids ratio became 1.17; in other words, the increase of pressure caused the volume of the voids to decrease by 0.50, representing a decrease in volume equal to 50 per cent of the volume occupied by the solids. Hence we are justified in stating that the clay is exceedingly compressible in comparison with the sand. On the other hand, if the

pressure which acts on the layer of sand is reduced from 3 to 0.5 kilogram per square centimeter, reversing the preceding process, it will be found that the voids ratio increases from 0.93 to 0.94, the increase of the volume of the voids being equal to about 1 per cent of the volume occupied by the solids. The same process of reducing the pressure on a layer of clay caused the voids ratio to increase from 1.17 to 1.30 (13 per cent of the volume occupied by the solid matter). Since the expansion of the soil produced by reducing the pressure represents the reversible part of the preceding compression, we say that the clay is far more elastic than the sand.

The compressibility and the elasticity of a soil can be visualized by plotting a diagram with the pressures as abscissas and the corresponding voids ratios as ordinates. Figure 1 shows such diagrams for eight different typical soils (full-lined curves). For each of these materials the compression test was started at the liquid limit (upper plastic limit), which approximately represents the voids ratio of the soil material when deposited by very slow sedimentation and it has not been subject to any pressure (external or capillary) except its own weight. The pressure acting on the sample was raised in succession from zero to 0.4, 0.8, 1.6, and 3.2 kilograms per square centimeter (approximately) and the voids ratio corresponding to each pressure was determined. With this data the compression curves were plotted. By reducing the pressure from 3.2 down to 1.6, 0.8, 0.4, and zero kilograms per square centimeter (approximately), the soil was allowed to swell, and the points representing the successive states of the expansion determine the swelling curve. From these diagrams it is easy to determine the volume of voids or the water content of the soil standing under a pressure of a given intensity. The steeper the compression curve, the more compressible is the soil, i. e., the greater is the volume change produced by loading the surface of the soil. On the other hand, the steeper the swelling curve, the more the soil will expand as a result of removing an external pressure. As a rule, a steep compression curve is associated with a steep swelling curve.

COMPRESSION OF SOILS REPRODUCED WITH SAND-MICA MIXTURES

The difference between the compression diagrams of the different soils is so striking that it could not fail to attract attention as soon as it was discovered. Since the compressibility of sand with only bulky grains is always, without exception, very small, very much smaller than that of the least compressible material represented in Figure 1, the writer suspected that great compressibility of any soil may be due to the presence of an appreciable percentage of scalelike particles. In order to check this hypothesis, the writer induced G. Gilboy, of the Massachusetts Institute of Technology, to investigate the compressibility and the expansion of differently proportioned mixtures of sand and mica flakes, both with a grain size of 0.5 millimeter. The results of these investigations were striking. By properly selecting the mica content of the sand it was possible to imitate both the compressibility and the elastic rebound of all the clay soils which thus far have been investigated. In Figure 1 the dotted lines represent the effect of raising the pressure up to 3 kilo-

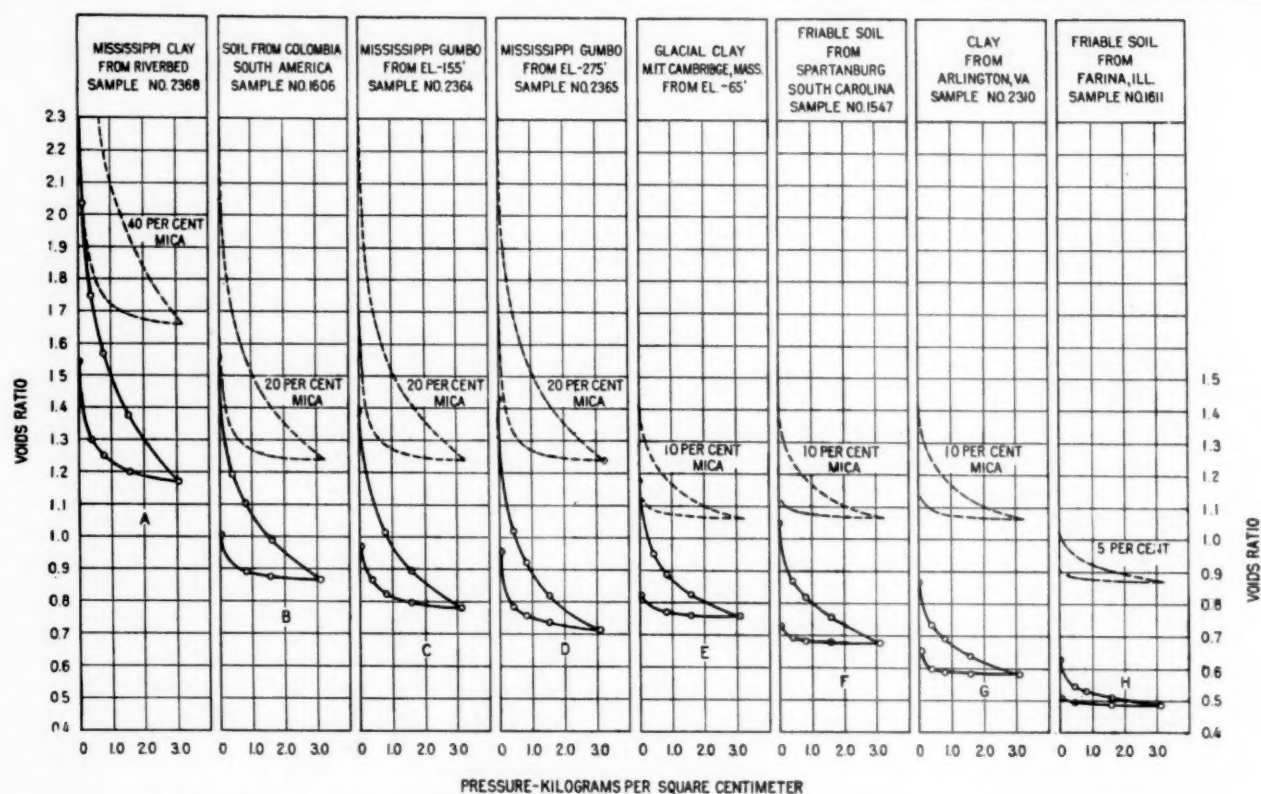


FIG. 1.—TYPICAL TIME-COMPRESSION CURVES FOR SOIL SAMPLES AND MIXTURES OF SAND AND MICA

grams per square centimeters and subsequently reducing it to zero on the particular sand-mica mixture which seemed to bear the closest resemblance to the soil whose compression curve is shown below. The soil curves are lower in the diagram than the sand-mica curves only because of the difference in uniformity of the two materials. As a rule, the more uniform a material is the greater is its volume of voids in a loose state.

Another difference between the curves representing soil and sand-mica is the range over which the two materials expand if completely relieved from pressure. Although the shapes of the expansion curves for both materials may be almost identical, the final expansion (due to removing the last pressure increment) is always very much smaller for the clays, than for the equivalent sand-mica mixtures. This is because the sand-mica mixture is perfectly cohesionless, the particles being free to move, while the clay always retains part of its cohesion, even after complete removal of the external pressure. (Fig. 1.)

It should be noticed that the voids ratio at the beginning of each test is in every case less for the clay soils than for the corresponding perfectly cohesionless sand-mica mixture. Since the initial voids ratio of the clay was always equal to or slightly above the liquid limit, we learn from Figure 1 that the liquid limit corresponds to at least as dense and as stable a mass as that of a well-shaken sand-mica mixture.

Figures 2 and 3 illustrate the difference in compressibility of various sand-mica mixtures. The upper row of pictures in Figure 2 show different mixtures, each weighing 200 grams and with mica contents of 0, 5, 10, 20, and 40 per cent, respectively. The lower row of pictures show the compression produced by a standard pressure of 1 ton per square foot.

Thus it became evident that the compressibility and elastic rebound of soils has very little to do with effective size, uniformity or colloid content. The controlling factor seems to be merely the mechanical effect of a greater or smaller abundance of scalelike particles.¹ In the final soil classification, which is on the point of being worked out, full advantage will be taken of this important fact.

GRAIN-SIZE CONTROLS SPEED OF COMPRESSION

The only difference between the results of compression tests performed on a clay soil and on an equivalent sand-mica mixture concerns the speed with which the decrease in volume takes place. Suppose the sand-mica mixture came to rest under a pressure

¹ This hypothesis was merely based on the similarity between the elastic properties of clays and of sand-mica mixtures. Facts however accumulate which seem to show that the clays really do contain a considerable percentage of scalelike particles. Some of them were published in the writer's book, *Erdbaumechanik*, Vienna 1925, which discusses plasticity of the powders of minerals which break up into scalelike particles, difference between the linear shrinkage of clay samples in the direction of the pressure exerted on the samples in pressing them into molds and the linear shrinkage perpendicular to this direction, etc. Quite recently C. S. Ross and E. V. Shannon succeeded in determining the physical form of the clay minerals of bentonite and related clays and found the following constituents: Montmorillonite (micaceous), beidellite (micaceous), micaceous halloysite (micaceous), halloysite (amorphous or submicroscopically crystalline), kaolinite (platy crystalline). "The minerals of bentonite and related clays and their physical properties," by C. S. Ross and E. V. Shannon. *Journal of the American Ceramic Society*, vol. 9, February, 1926. Thus out of five clay minerals contained in bentonite, three are micaceous, one platy crystalline, and only one is apparently amorphous. The elasticity (elastic rebound) of average clays corresponds to the elasticity of a sand-mica mixture with 10 per cent mica and those of the most elastic clays to mixtures with 20 per cent mica. Hence the findings of Ross and Shannon represent an important step towards explaining the similarity between clays and sand-mica mixtures.

There exists, however, one more group of soil constituents, which seem to have an effect on the elasticity of the soils very similar to the effect of mica. This group consists of the organic colloids. One year ago the writer showed, that the compression curve of gelatine is almost the same as the compression curve of an accumulation of mica flakes. The difference between the gelatine and the mica powder merely consists in the fact that the gelatine is almost perfectly elastic the expansion curve being almost identical with the compression curve, whereas the mica powder is imperfectly elastic, as are all accumulations of individual grains. From what we know thus far, a high content in organic matter associated with mica content (silts) causes considerable elasticity and an abnormally high liquid limit combined with a comparatively low plasticity index.

of 1.5 kilograms per square centimeter. If the pressure is increased rapidly from 1.5 to 3 kilograms per square centimeter, from 90 to 95 per cent of the compression takes place almost at once. Then the compression slowly increases as time goes on and after a couple of hours, equilibrium is practically reached, and the compression proceeds no further. Figure 4, A shows the results of time observations made on a layer of a 20 per cent sand-mica mixture. When making the same test on a clay with equal compressibility, practically none of the compression takes place at once, the time required for obtaining 75 per cent of the total compression depending on both the permeability of the material and the thickness of the layer. Figure 4, B shows the time-compression curve for a highly plastic soil from Colombia, South America, and Figure 4, C shows an equally plastic gumbo from the bed of the Mississippi River. The compressibility of these three materials is shown in Figure 1, A, B, and C. Since all three materials are practically equally compressible and elastic, it seems logical to associate the differences between the time-compression curves with differences in grain-size of the materials.

If the mechanics of the process of consolidation under pressure is considered, it at once becomes obvious that a low degree of permeability must be associated with slow consolidation. Suppose a 20-centimeter layer of a material with the compressibility of the soils in Figure 4 be subject to a rapid increase in pressure from 1.5 to 3.1 kilograms per square centimeter, resulting in a decrease in thickness of 1.4 centimeters. If the voids of the material are filled with air only, the compression of the layer from 20 to 18.6 centimeters can take place at once, except for the time required for the particles to adjust themselves to the modified conditions of stress within the layer. In cases like that of Figure 4, A, the lag is insignificant. On the other hand, if the voids of the material are filled with water, compression from a thickness of 20 centimeters down to 18.6 centimeters requires a sheet of water 1.4 centimeters thick to flow from the interior of the material through its upper surface. No water can flow unless there is a hydraulic gradient, and the less permeable the material, the slower will be the flow under a given gradient. Hence, the time required to press a sheet of water 1.4 centimeters thick out of the material will depend on how permeable the material is.

The mechanics of the lag in compression can best be learned by discussing an apparatus as illustrated in Figure 5. Figure 5, A, represents a cylindrical vessel with a perforated piston the weight of which is compensated by the pressure exerted by two springs, S_1 and S_2 . If the space below the piston is empty, a pressure applied on top of the piston will cause the piston to move almost instantaneously downward through a distance, d , depending on the compressibility of the springs. On the other hand, if the space below the piston is filled with water, the downward movement of the piston will be retarded on account of the time required for the water to escape through the openings of the piston. The smaller the openings, the longer it will take the piston to reach its final position. During the downward movement, the water located beneath the piston will be under a pressure the intensity of which depends on the hydraulic gradient required to force the water through the openings. The longer the pressure acts, the lower the speed with which the water escapes, and finally the system will come to

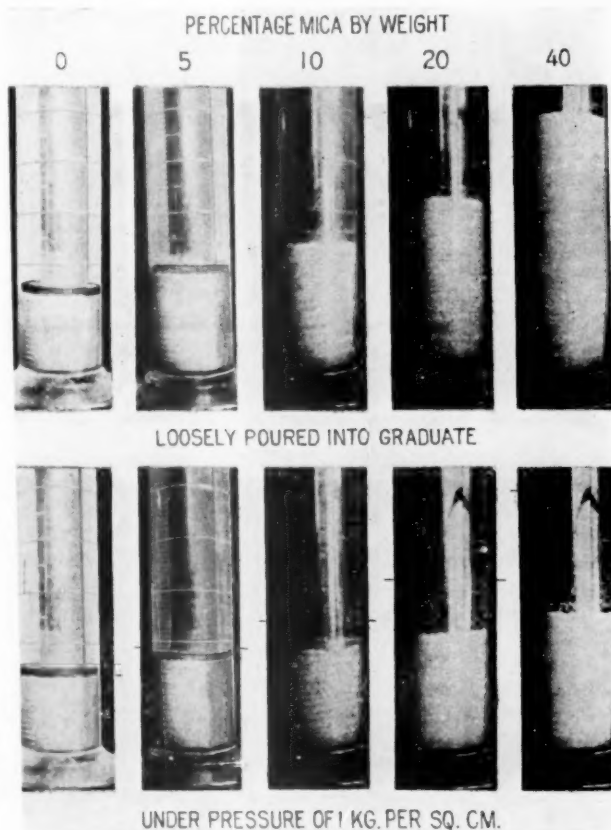


FIG. 2.—ACTUAL SAMPLES OF SAND-MICA MIXTURES SHOWN DIAGRAMMATICALLY IN FIGURE 3

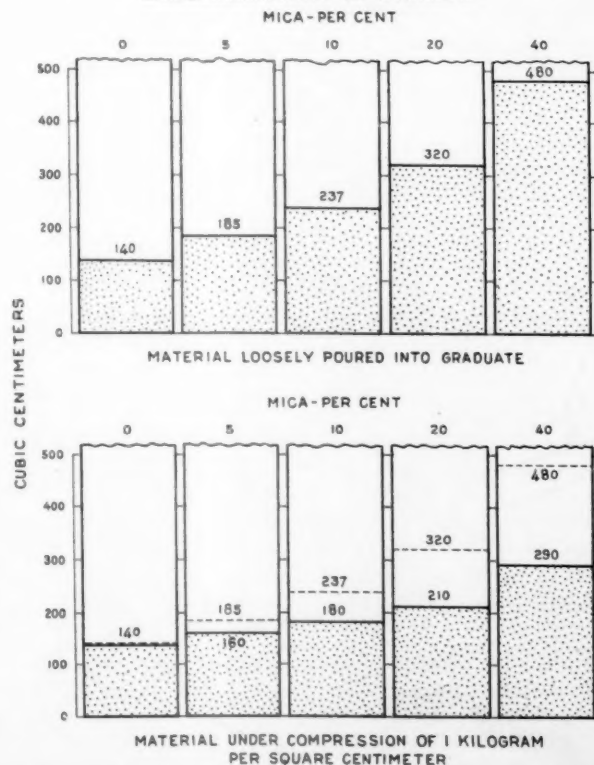


FIG. 3.—COMPRESSION PRODUCED BY A PRESSURE OF 1 KG. PER SQ. CM. ON 200 GM. SAMPLES OF VARIOUS SAND-MICA MIXTURES

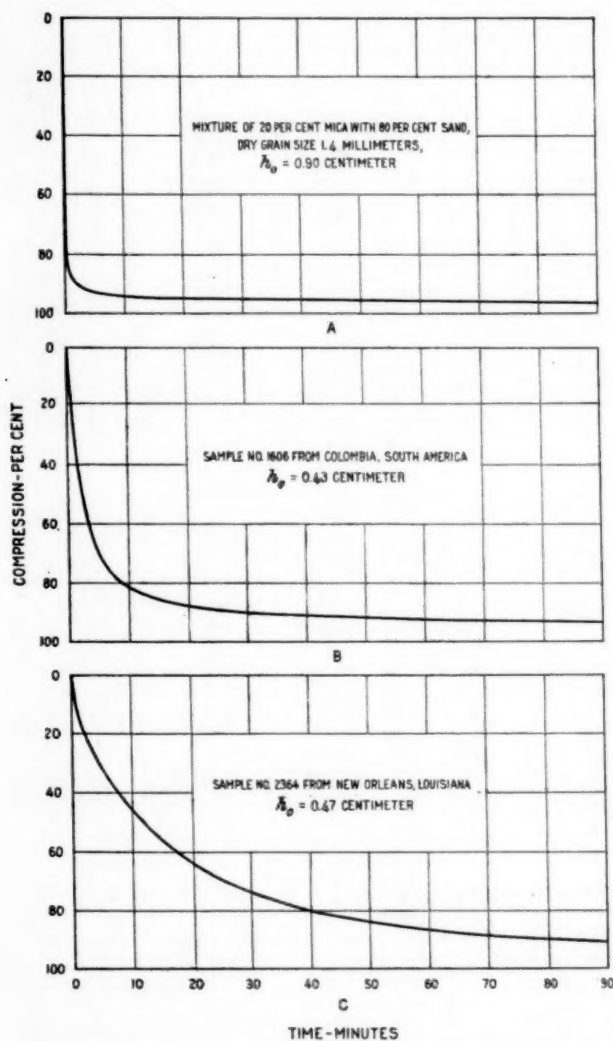


FIG. 4.—COMPARISON OF TIME-COMPRESSION CURVES FOR A 20 PER CENT SAND-MICA MIXTURE AND TWO SOILS. COMPRESSION PRODUCED IN 17 HOURS BY RAISING PRESSURE FROM 1.58 TO 3.10 KG. PER SQ. CM. IS TAKEN AS 100 PER CENT

rest and the hydrostatic pressure in the water beneath the piston becomes equal to zero.

The water contained in the voids of a water-soaked, compressible layer of soil (fig. 5, B) behaves under pressure in precisely the same manner as does the water beneath the piston of Figure 5, A. The only difference is that in the case of Figure 5, B, the obstacles which interfere with the escape of the water are scattered throughout the space; hence, the hydrostatic excess pressure will be different in different parts of the layer. Nevertheless, the size of the openings still remains the principal factor controlling the speed with which the water escapes.

MATHEMATICAL RELATION EXISTS BETWEEN PERMEABILITY AND SPEED OF COMPRESSION

Since the speed of the process of consolidation depends on nothing but the quantity of water to be forced out of the soil and on the resistance against flow of the water through the material, it has been possible to work out a theory of consolidation of water-soaked soils under pressure and to compute the permeability from the speed with which consolidation

proceeds. Since this theory has been published elsewhere² the results only are presented here. Let

h_0 be the reduced thickness of the layer of soil in centimeters, i. e., the thickness the layer would have at a volume of voids equal to zero.

p_0 the pressure acting on the sample before the beginning of the test in grams per square centimeter.

$p_0 + p_1$ the pressure acting on the sample during the test, in grams per square centimeter.

t the elapsed time in minutes after the pressure was raised from p_0 to $p_0 + p_1$.

e_0 the voids ratio of the sample at the beginning of the test.

e the voids ratio of the sample after time t .

e_1 the voids ratio of the sample after an infinite time.

$\Delta e = e_0 - e$ the compression after a time t .

$\Delta e_1 = e_0 - e_1$ the final compression produced by increasing the pressure from p_0 to $p_0 + p_1$.

(Since the voids of the soil are supposed to be completely filled with water, the voids ratio, e , is synonymous with the water content in cubic centimeters per cubic centimeter of solid soil material.)

$a = \frac{\Delta e_1}{p_1}$ (p_1 in grams) the coefficient of compressibility, i. e. the average decrease in voids ratio produced per gram of additional pressure.

Finally, the speed, with which the process of consolidation proceeds depends on the value of k , the coefficient of permeability. To explain the meaning of the coefficient of permeability, let us suppose a layer of soil with a thickness, h , inclosed between two vertical screens. (Fig. 6, A.) Through each of these screens the voids of the soil are supposed to communicate with bodies of free water. If the water on the left side of the soil stands higher than on the right side, the water percolates through the soil from the left to the right. According to Darcy's law the speed of percolation increases in direct proportion with the hydraulic gradient (ratio between the difference in water pressure on both sides of the layer of soil and the distance through which the water percolates, which in this case, is equal to the thickness, h , of the layer). If the difference in elevation of the two water levels is equal to h , the thickness of the layer, the hydraulic gradient is equal to unity. The speed of percolation at a hydraulic gradient equal to unity is called the coefficient of permeability k_1 . It should, however, be noticed, that the speed of percolation does not indicate the velocity with which the water moves through the voids of the soil, but the speed with which it moves immediately after it leaves the soil, through the unobstructed space adjoining the downstream screen. Hence the speed of percolation expresses as well the quantity of water which passes per unit of time through a unit of area of the layer.

What precedes represents the current definition of the coefficient of permeability. It refers to the true thickness of the layer of soil. In contrast to this, in the computations concerning the consolidation of soils we are obliged to refer everything to the reduced dimensions of the samples; that means to the thickness the samples would have if the space occupied by the voids were reduced to zero. Otherwise it would be impossible mathematically to solve the equations. The reduced thickness of the sample has been called h_0 . The true thickness, h , is equal to $h_0 (1 + e)$ wherein e is the voids ratio.

² TERZAGHI, CHARLES. DIE BERECHNUNG DER DURCHLÄSSIGKEITZIFFER DER TÖNE AUS DEM VERLAUF DER HYDRODYNAMISCHEN SPANNUNGSERSCHEINUNGEN. Sitzungsberichte der Akademie der Wissenschaften in Vienna, mathem. naturw. Klasse, Abt. II a, pp. 125-138, 1923. A short abstract appeared in Engineering News-Record, Nov. 26, 1923.

The reduced coefficient of permeability, k , is the speed with which the water would percolate through the sample if the difference between the two water levels were h_0 instead of h . This speed of percolation is obviously smaller than the true coefficient of permeability. Since, according to Darcy's law, there exists

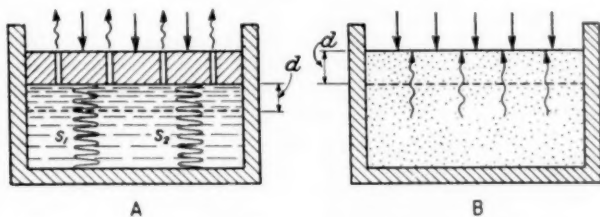


FIG. 5.—APPARATUS ILLUSTRATING ACTION OF WATER UNDER HYDROSTATIC PRESSURE, ESCAPING THROUGH SMALL OPENINGS

a simple proportionality between the hydraulic gradient and the speed of percolation, we can write

$$k_1 : k = \frac{h}{h_0} : \frac{h_0}{h} = 1 : \frac{1}{1+e}$$

$$\text{Hence } k = \frac{k_1}{1+e}$$

When making the standard compression test, the water percolates through the sample—not in a horizontal direction, as shown in Figure 6, but in a vertical direction. After the pressure has been raised from p_0 to $p_0 + p_1$, the voids ratio decreases from e_0 to $e_1 = e_0 - \Delta e_1$. The average voids ratio during this process is $e = \frac{e_0 + e_1}{2} = e_0 - \frac{\Delta e_1}{2}$. In introducing this value of e into our formula we obtain for the reduced coefficient of permeability the formula

$$k = \frac{k_1}{1 + e_0 - \frac{1}{2}\Delta e_1}$$

While the voids ratio of the sample decreases from e_0 to e_1 , both the true and the reduced coefficient of permeability decrease. At the same time the value of the coefficient of compressibility decreases, the aforementioned value, a , merely representing the average for the whole range from e_0 to e_1 . Fortunately the fundamental equations contain neither the value of k nor the value, a , individually, but they contain the ratio between these two values, viz, $c = \frac{k}{a}$. This value is called the coefficient of consolidation. While both the values of a and of k rapidly decrease with the voids ratio, the variations of c are far less significant, which fact considerably increases the degree of accuracy of our computations.

To make the list of symbols used in the following equations complete, we have, as a result of the preceding discussions, to add

k_1 the coefficient of permeability of the soil in cm. per min., or the velocity with which the water flows through the soil under a hydraulic gradient equal to one,

$k = \frac{k_1}{1 + e_0 - \frac{1}{2}\Delta e_1}$ the reduced coefficient of permeability, and

$c = \frac{k}{a}$ the coefficient of consolidation.

By theory it was found that the aforementioned quantities are connected with each other by the following equation:

$$\Delta e = \Delta e_1 \left[1 - \frac{8}{\pi^2} e^{-\frac{c\pi^2}{4h_0^2}t} - \frac{8}{9\pi^2} e^{-\frac{9c\pi^2}{4h_0^2}t} - \dots - \frac{8}{(2n+1)^2\pi^2} e^{-\frac{(2n+1)^2c\pi^2}{4h_0^2}t} \right] \quad (1)$$

Figure 7 shows this relation graphically, for a material with $\Delta e_1 = 100$ per cent and $\frac{c\pi^2}{4h_0^2} = 1$. The effect of the assumption $\frac{c\pi^2}{4h_0^2} = 1$ will be discussed later. In Figure 8

the results of time observations with gelatine have been plotted. The small circles represent the results of the measurements and the full line shows the theoretical consolidation curve according to the preceding equation. Since the internal friction in gelatine is very small, the agreement between theory and observation is almost perfect.

PERMEABILITY COMPUTED FROM TIME OBSERVATIONS

When a layer of water-soaked soil consolidates under pressure, the time effect due to low permeability combines with the time effect due to internal friction. According to equation (1) the time effect due to low permeability increases in direct proportion with the square of the reduced thickness h_0 of the layer. In contrast to this, the time effect due to internal friction (gradual adjustment of the soil particles) was found to be practically independent of the value of h_0 . Hence interpretation of the time-compression curves representing test results is apt to be misleading unless one succeeds in separating the two effects from one another. This can be done on account of the fact that if there were no appreciable resistance against the escape of the water, the first part of the compression would occur almost instantaneously.

In the following discussion this part will be called $n\Delta e_1$, the value of the coefficient, n , ranging according to the type of the soil and to the value of p_0 anywhere between 0.6 and 1 (60 and 100 per cent). As a rule, the value of n is about 0.85 (more or less). The second part $(1-n)\Delta e_1$ represents the compression due to gradual adjustment of the grains and the speed with which this part of the compression takes place, is essentially governed by internal friction (friction between the soil grains). Hence if there is an appre-

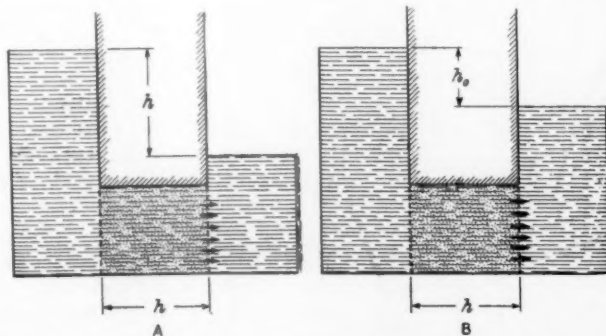


FIG. 6.—DIAGRAMS USED IN DEFINING MEANING OF k_1 THE COEFFICIENT OF PERMEABILITY AND k THE REDUCED COEFFICIENT OF PERMEABILITY

ciable lag between $\Delta e = 0$ and $\Delta e = n\Delta e_1$ this lag is almost exclusively due to the resistance against the flow of the water. The shape of the curve for the lag due to low permeability is very characteristic. Due to this fact the problem merely consists in finding out how far the time-compression curve follows the law expressed by equation 1 and in determining the con-

stants of this first section of the curve. To solve this problem a simple graphical method has been devised.

This method is based on the following facts: Let

Δe be the compression produced by increasing the pressure from p_0 to $p_0 + p_1$, after a time t_1 (fig. 7),
 $\Delta e_1 = 100$ per cent compression, the compression after an infinite time, and
 t_2 the time required to produce the compression $\frac{\Delta e}{2}$ (fig. 7).

If the values of Δe are plotted as ordinates and the corresponding values of $\frac{t_1}{t_2}$ as abscissas (curve C in fig.

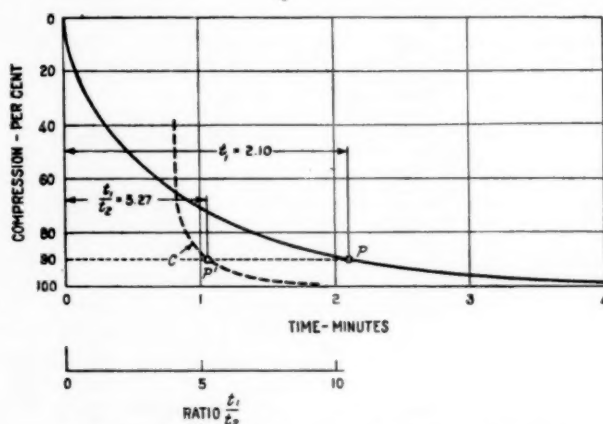


FIG. 7.—THEORETICAL TIME-COMPRESSION CURVE

7) a curve is obtained with a very characteristic shape.

From $\Delta e = 0$ up to $\Delta e = 0.7\Delta e_1$ the value of $\frac{t_1}{t_2}$ is approximately equal to 4, which means that within this range, the consolidation curve is approximately a parabola.

Between $\Delta e = 0.7\Delta e_1$ and $\Delta e = 0.94\Delta e_1$ the value of $\frac{t_1}{t_2}$ increases from 4 to 6, and between the limits of $\Delta e = 0.94\Delta e_1$ and $1.00\Delta e_1$ it goes rapidly up from 6 to infinity.

When comparing theoretical curves of the type of Figure 7 with the actual time-compression curves for a considerable number of soils the following fact was noticed. As a rule, the empirical curves have very nearly the same shape as the theoretical curves up to a point which, on the theoretical curve, has an ordinate of 90 per cent (approximately). Beyond this point the discrepancy between the two curves increases very rapidly, in such a manner, that the 100 per cent ordinate of the theoretical curve corresponds to an ordinate n equal to anywhere between 80 and 100 per cent on the actual curve. An ordinate of 90 per cent ($\Delta e = 0.90\Delta e_1$) on the theoretical curve corresponds to a value of $\frac{t_1}{t_2}$ of 5.27.

Hence, in order to adapt equation 1 to an empirical time-compression curve (see, for example, the curves of fig. 9, soil No. 2250), we start by tracing a short section of the $\frac{t_1}{t_2}$ curve (dotted curve C in fig. 9, B to E) and determine on this curve the point P_1 for which the value of $\frac{t_1}{t_2}$ is equal to 5.27. Then we find the point P on the consolidation curve whose ordinate is equal to the ordinate of P_1 . The point P corresponds to the point P on the consolidation curve, Figure 7, and also to the time t_1 in the consolidation diagrams, Figure 9.

If there were no internal friction in the soil, the consolidation would occur according to a theoretical curve

which passes through the point P and which approaches a horizontal asymptote with an ordinate, n , equal to $\frac{1}{0.90}$ times the ordinate of the point P . The problem merely consists in determining the value of c for which the theoretical curve passes through the point P with an abscissa t_1 and an ordinate 90 per cent.

In order to solve this problem we return to equation 1. In Figure 7 the point P with an ordinate 90 corresponds to an abscissa $t_1 = 2.1$. If we introduce in equation 1 the data for point P in Figure 7, viz,

$\frac{c\pi^2}{4h_0^2} = 1$ and $t_1 = 2.1$, we obtain:

$$\Delta e = \Delta e_1 \left[1 - \frac{8}{\pi^2} e^{-1 \times 2.1} - \frac{8}{9\pi^2} e^{-9 \times 1 \times 2.1} - \dots - \frac{8}{(2n+1)^2 \pi^2} e^{-(2n+1)^2 \times 2.1} \right] = 0.9\Delta e_1.$$

If we had plotted our curve (fig. 7) for any other value of $\frac{c\pi^2}{4h_0^2}$, for instance, $\frac{c\pi^2}{4h_0^2} = 5$, we would have obtained

for t_1 the value $t_1 = \frac{2.1}{5} = 0.42$ simply because our equation does not furnish the result $\Delta e = 0.9\Delta e_1$, except for one definite value of the exponent of e . Hence, if for $\frac{c\pi^2}{4h_0^2}$ we assume a value of 5 instead of 1 then the value of t_1 would become $\frac{2.1}{5}$, and we have

$$-(2n+1)^2 \times 1 \times 2.1 = -(2n+1)^2 \times 5 \times \frac{2.1}{5}, \text{ etc.}$$

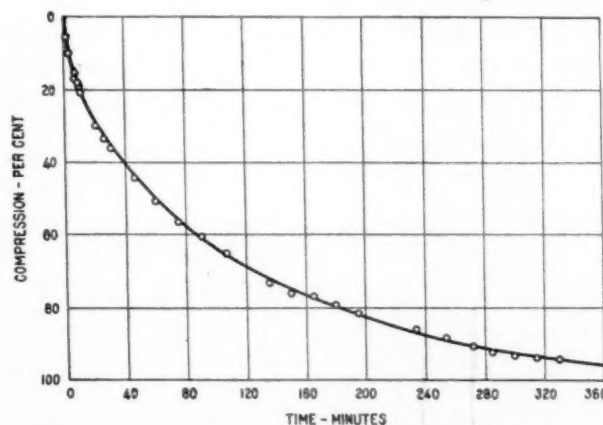


FIG. 8.—FULL LINE REPRESENTS THEORETICAL CURVE WHILE CIRCLES SHOW CLOSE AGREEMENT OF TEST ON ISOELECTRIC GELATINE, LOWERING THE PRESSURE FROM 11.1 TO 5.57 KG. PER SQ. CM. THE TIME OF TEST WAS ONE WEEK. THE TEST WAS ACTUALLY MADE BY ALLOWING THE GELATINE TO EXPAND RATHER THAN COMPRESSING IT, BUT SINCE GELATINE IS ALMOST PERFECTLY ELASTIC THERE IS PRACTICALLY NO DIFFERENCE BETWEEN COMPRESSION AND EXPANSION CURVES

In Figure 9 the abscissa t_1 is determined by the test results. Since, according to what precedes, for $\Delta e = 0.9\Delta e_1$, the product $\frac{c\pi^2}{4h_0^2} t_1$ must be equal to 2.1, we can write the equation

$$\frac{c\pi^2}{4h_0^2} t_1 = 2.1$$

or the factor of consolidation of our sample

$$c = \frac{2.1 \times 4}{\pi^2} \times \frac{h_0^2}{t_1} = 0.85 \frac{h_0^2}{t_1} \quad (2)$$

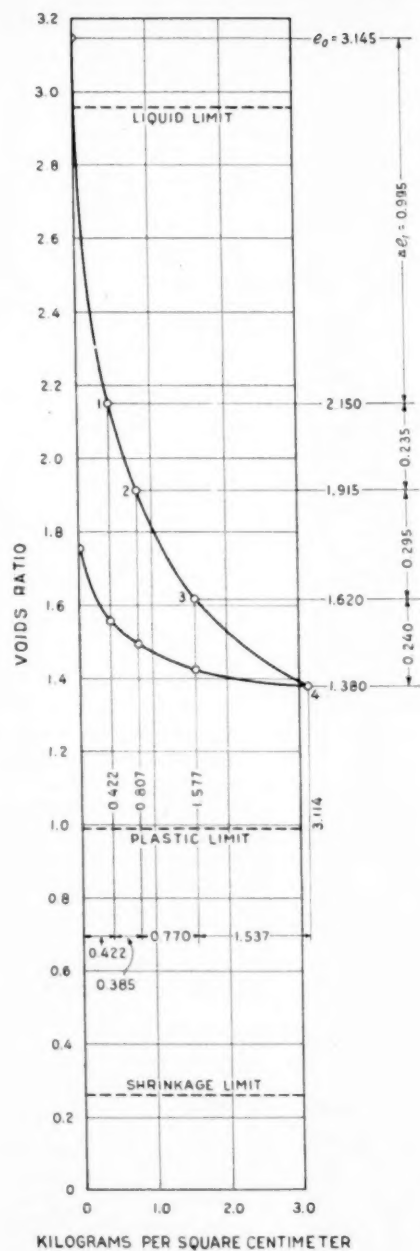
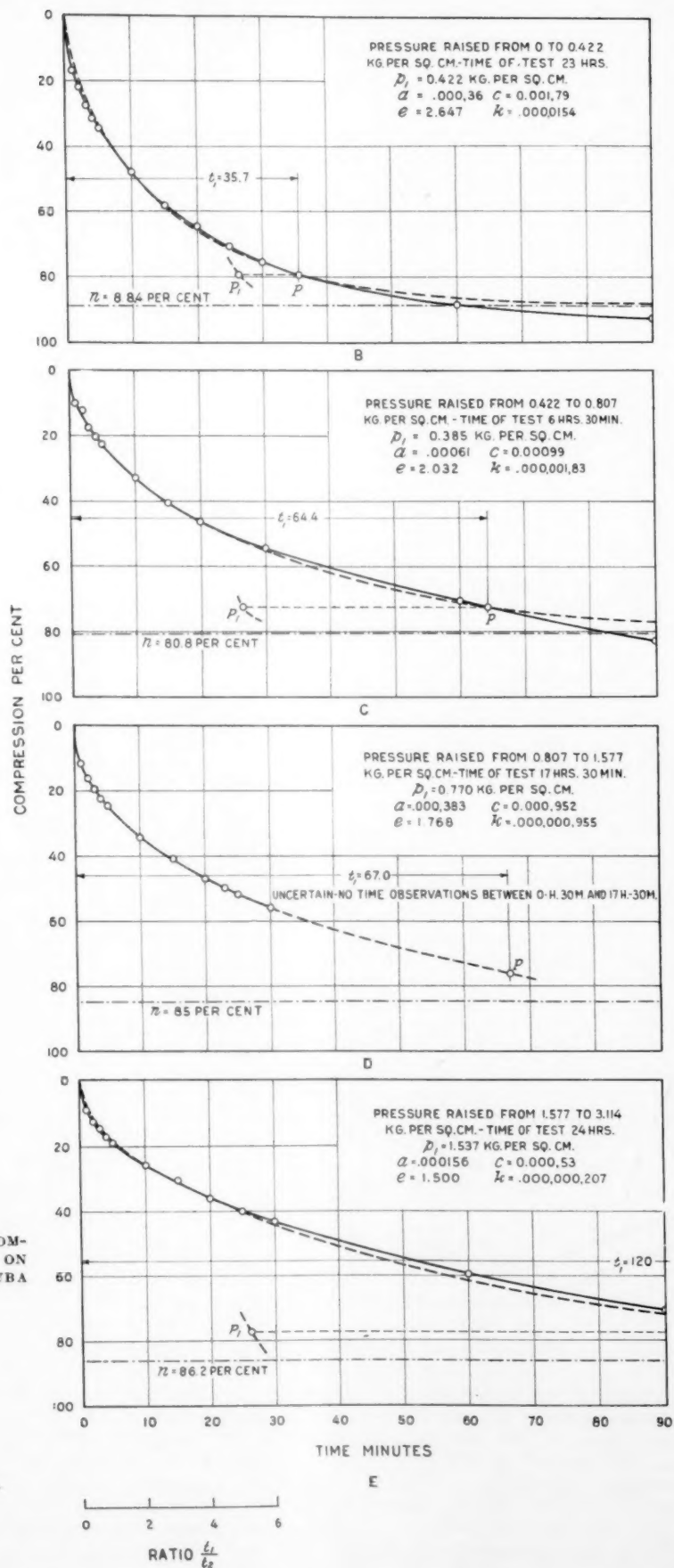


FIG. 9.—Load-compression curve and time-compression curves as a result of tests on sample No. 2250, YAGUAJAY CLAY FROM CUBA



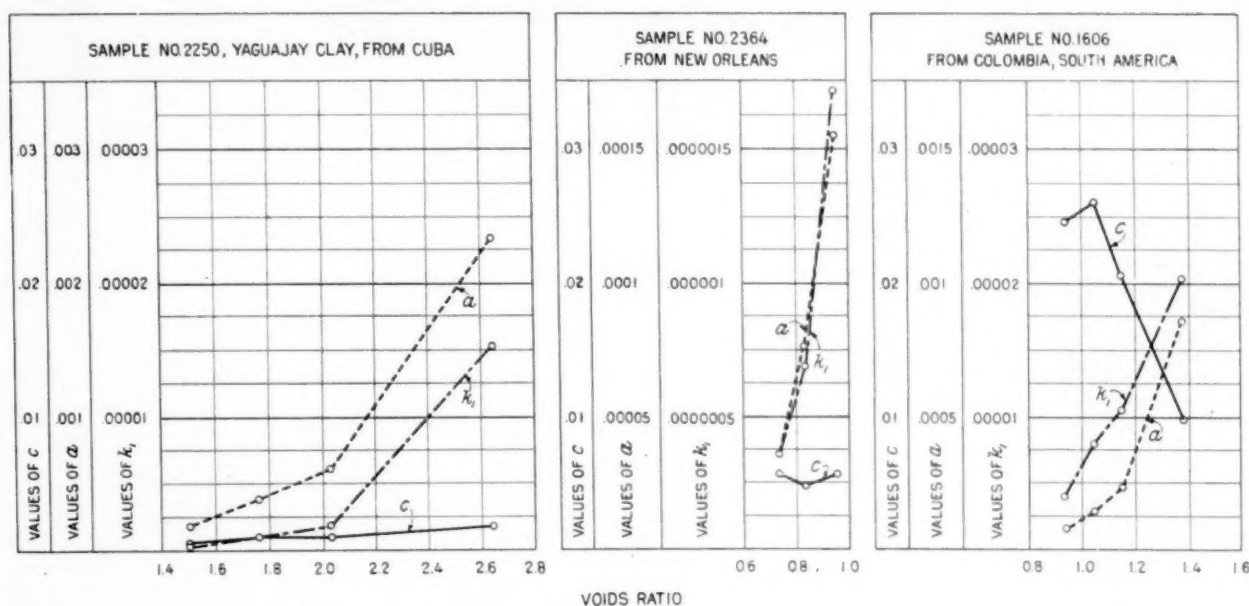


FIG. 10.—CURVES SHOWING VARIATION IN VALUE OF c , a , AND k_1 , FOR THREE TYPICAL SOIL SAMPLES

wherein h_0 is the reduced thickness of our sample in centimeters (see nomenclature for equation 1) and t_1 is the time in minutes which corresponds to point P on the consolidation curve.

The value of c being determined, it remains to consider how to find the value of k_1 (coefficient of permeability). Strictly speaking, the value c derived from any time-compression curve represents the average coefficient of consolidation for the range e_0 to $e_0 - n\Delta e_1$. In addition to this, the following fact should be kept in mind: According to Figure 9, the lag due to low permeability occurs, as if the compression of the sample were equal to $n\Delta e_1$, the corresponding coefficient of compressibility being equal to $\frac{n\Delta e_1}{p_1}$ instead of $\frac{\Delta e_1}{p_1}$.

However, considering the errors involved in the graphical procedure as such and the degree of accuracy required for classification purposes, these facts are disregarded, except when making investigations for scientific purposes. For current work we refer all the values resulting from the computation for any specific pressure interval p_0 to $p_0 + p_1$ to the voids ratio $e_0 - \frac{1}{2}\Delta e_1$ (average voids ratio for the time-compression process) and consider the coefficient of compressibility equal to

$\frac{\Delta e_1}{p_1}$. On this assumption we obtain

$$a = \frac{\Delta e_1}{p_1}, \quad k = ca, \quad \text{and} \quad k_1 = ca(1 + e_0 - \frac{1}{2}\Delta e_1).$$

METHOD ILLUSTRATED BY EXAMPLE

As an example of what precedes, Figures 9 and 10 may serve. Figure 9, A, shows the pressure-voids ratio curve for a highly plastic clay from Cuba and the Figures 9, B to E, the results of the time-pressure observations. The pressure was raised by increments from zero to 0.422, 0.807, 1.577 and 3.114 kilograms per square centimeter. The corresponding values of p_1 and Δe_1 can be learned from Figure 9, A. They are as well represented in Table 1. This table shows in addition the numerical computations in the order in

which they follow each other. The data for computing the values contained in the lines 1 to 5 of the table are obtained from the pressure-voids ratio diagram Figure 9, A. The next step consists in determining the value t_1 . For this purpose one first traces a smooth curve through those points in the time-compression diagram, which represent the actual observations. In the diagrams, this curve is shown by a full line. Then one plots the curve C , whose abscissas represent the values of t_1 . With some skill one usually succeeds in obtaining the information required by plotting not more than three points on this curve. The point whose abscissa is $t_1 = 5.27$ represents point P_1 . The abscissa of the point P which corresponds to the point P_1 on the t_1 -curve gives the value t_1 in the table.

For the purpose of checking the actual observations against the theoretical values determined by equation 1 the following procedure can be followed: In Figure 7 the ordinates 0.2, 0.4, 0.6, 0.8, 0.90, and 0.95 (20, 40, etc., if expressed as a percentage) correspond to the abscissas (values of t_1) 0.08, 0.316, 0.70, 1.42, 2.10, and 2.80. In the time-compression diagram (fig. 9), the ordinate of the horizontal asymptote to the theoretical curve is equal to n , equal to $\frac{1}{0.90}$ times the ordinate of point P . Hence, in order to trace the theoretical curve through the point P in Figure 9, divide the space between zero and n into equal parts, such as to obtain on the vertical axis points with the ordinates $0.2n$, $0.4n$, $0.6n$, $0.8n$, and $0.95n$. Since the difference between the theoretical curves in Figure 7 and Figure 9 is one of scale only, the abscissas of P being equal to 2.1 and t_1 , respectively, the abscissas of the theoretical curve in Figure 9, for the ordinates $0.2n$, $0.4n$, $0.6n$, $0.8n$, $0.90n$ and $0.95n$ will obviously be equal to $\frac{0.08}{2.1}t_1$, $\frac{0.316}{2.1}t_1$, $\frac{0.70}{2.1}t_1$, $\frac{1.42}{2.1}t_1$, $\frac{2.80}{2.1}t_1$ and t_1 . In the time-compression diagrams Figure 9, B to E, the theoretical curves thus obtained are shown by dotted lines.

TABLE 1.—Computation of coefficients of consolidation and permeability for sample No. 2250 for four increments of load with $h_0 = 0.27 \frac{1}{4}$ cm.

	First load increment	Second load increment	Third load increment	Fourth load increment
p_1 in grams per square centimeter	422	385	770	1,537
e_0	3.145	2.150	1.915	1.620
Δe_1	0.995	0.235	0.295	0.240
$e = e_0 - \frac{\Delta e_1}{2}$	2.647	2.032	1.768	1.500
$a = \frac{\Delta e_1}{p_1}$	0.00236	0.00061	0.000383	0.000156
t_1 in minutes	35.7	64.4	67.0	120.0
n	0.88	0.81	0.85	0.86
$c = 0.85 \frac{h_0^2}{t_1} = 0.0638$	0.00179	0.00099	0.00095	0.00053
$k_1 = \frac{c}{a(1+e)}$	0.0000154	0.0000183	0.0000096	0.0000021

After the values of t_1 have been found, the values of c and k_1 can be computed (lines 8 and 9 in Table 1). Figure 10, A shows the results of the computations graphically, the values of a , c and k_1 plotted against voids ratio. Figure 10, B and C, represent similar test results for two other soils.

These diagrams bring out the known fact that the coefficient of permeability decreases very rapidly with decreasing voids ratio. The same is true for the coefficient of compressibility. Coefficients as variable as these are certainly not suitable for classification purposes. On the other hand, the degree of permeability of a soil is a property of such far-reaching and universal importance that no classification for engineering purposes can be satisfactory without considering it. The simplest way to overcome the difficulty is to express it indirectly, by the average coefficient of consolidation. Figure 10 indicates that the coefficient of consolidation is far less variable than either a or k_1 , and at the same time it depends directly on permeability. The coefficient of consolidation of soils varies from less than 0.001 for very plastic clays to 500 or more for very fine sands. Hence no great accuracy in computing and expressing this coefficient is required for characterizing the soils.

It is proposed to make not more than two sets of time observations for every standard volume-compression test, one for raising the pressure from 0.4 to 0.8 kilogram per square centimeter approximately and one from 1.5 to 3 kilograms per square centimeter approximately and to consider the average coefficient of consolidation to be equal to the mean of these two values, omitting all decimals. The coefficient of consolidation for the first pressure increment from zero to 0.4 kilogram per square centimeter is disregarded, because this coefficient has been found to be usually an abnormal one, being excessively low or excessively high (fig. 10, A and B). Thus, for the three soils represented in Figure 10, the coefficients of consolidation would be equal to one-half $(0.00099 + 0.00053) = 0.0008$ for sample No. 2250, 0.005 for sample No. 2364, and 0.02 for sample No. 1606, these figures representing the order of magnitude of the coefficients.

COEFFICIENT OF CONSOLIDATION IS OF PRACTICAL SIGNIFICANCE

It is believed that the coefficient of consolidation is of considerable practical significance. Suppose we have two equally compressible clay soils, A and B, soil A with a coefficient of consolidation of 0.001, and soil B with a coefficient of consolidation of 0.1. If a similar load is placed on top of each of these soils the compression will be produced one hundred times more

rapidly in soil B than in soil A. Or, if the surface of both soils be simultaneously exposed to the air, so that the water can gradually evaporate, the dry crust which forms on soil B will be very much thicker than the dry crust on soil A. Finally, if both soils come into contact with open water, after having previously dried out, the soil B will swell one hundred times more rapidly than will the soil A.

It has been indicated that the value of the coefficient of consolidation ranges between extraordinarily wide limits. Since this coefficient determines the speed with which a pressure is apt to compress the soil, provided its voids are filled with water, it ranks among the most characteristic constants of the soil.

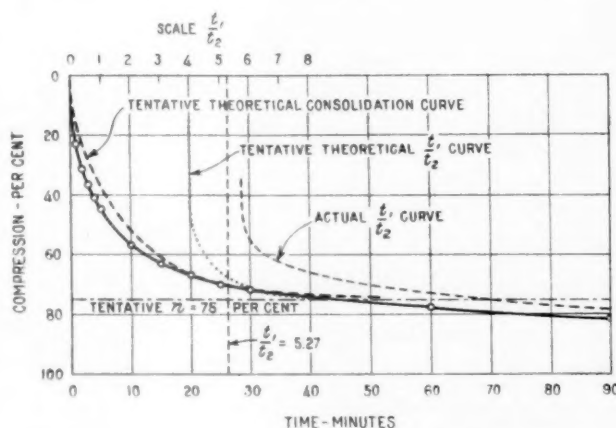


FIG. 11.—AN ABNORMAL CONSOLIDATION CURVE SHOWING CONSIDERABLE DEPARTURE FROM THEORETICAL CURVE. CURVE REPRESENTS COMPRESSION ON RAISING PRESSURE FROM 1.577 TO 3.114 KG. PER SQ. CM.

For friable soils consolidation is apt to proceed so rapidly that the time observations can not be made with the same degree of precision as can be done for slowly consolidating materials. In that case, a simple modification of the test arrangement makes it possible to obtain the data concerning the permeability of the material independent of the time-compression observations. The modification consists in compressing the material by means of a piston with a permeable bottom instead of using a piston with a watertight bearing surface. The permeability of the sample is computed from the speed with which the water flows from a narrow standpipe through the sample and through the permeable bottom of the piston into the hollow interior of the piston, while the sample is under pressure. The test results combined with the data furnished by the compression observations determine the value of the coefficient of consolidation.

The same procedure should be followed in those cases where the consolidation curve has an abnormal shape, that means where the value of n is smaller than approximately 0.8, a condition which seems to be quite common with feebly compressible soils with a low coefficient of permeability. In these cases the shape of the entire curve may considerably differ from the normal shape of the consolidation curve, as shown in Figure 11. This abnormality seems to be due to the finer fraction expanding into the larger voids while consolidation proceeds. The interpretation of the time-compression curve obtained under such conditions leads to values which are too high for the coefficients of consolidation and of permeability.

Hence, in order to determine the coefficient of consolidation two different procedures should be followed, depending on the character of the consolidation curve. If n is equal to or greater than approximately 0.80, and if in addition the value of t_1 for $\Delta e = 0.70 \Delta e_1$, is greater than five minutes, the coefficient of consolidation can be computed from the consolidation curve. Otherwise, the coefficient should be determined from the results furnished by the modified test arrangement.

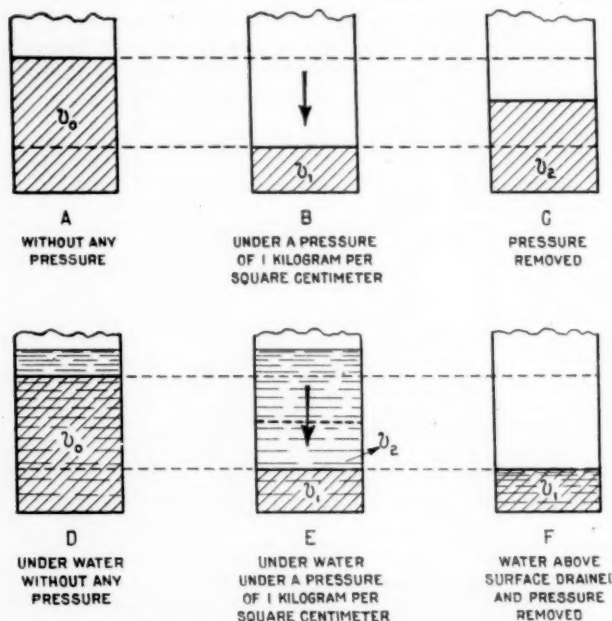


FIG. 12.—VOLUME CHANGE OF COTTON UNDER ORDINARY AND CAPILLARY PRESSURE

ACTION OF CAPILLARY PRESSURE ON POROUS MATERIAL INVESTIGATED

Thus far, we have merely considered the volume change of the soils (compression or expansion) produced by a change of the external pressure. It is known, however, that fine-grained soils such as clays and loams may change their volume apparently without any external pressure acting upon them. It is sufficient to expose them to the air to make them shrink, and subsequent wetting causes them to expand (swell). Until a short time ago it was generally assumed that shrinking and swelling were due to somewhat inexplicable properties of the colloids contained in fine-grained soils. Recent investigations, however, seem to show that the causes of shrinkage and swelling are very much simpler and that they reside in the action of no other forces than those which drive the water up in capillary tubes or in similar narrow channels. In order to visualize the action of these forces, let us first consider the behavior of a piece of cotton or of a very fine-grained sponge, subjected to an external pressure. Suppose cotton or sponge is put into a vessel (fig 12, A) with no load acting on top of it. For this state the material occupies a certain volume V_0 regardless of whether it is dry or completely immersed in water. Under the influence of a pressure of, say, 1 kilogram per square centimeter the volume goes down from V_0 to V_1 (fig. 12, B) again regardless of whether the sample is dry or completely immersed. We say that we have compressed the material. Finally, if the

pressure is removed, the volume goes up from V_1 to V_2 , smaller than V_0 (fig. 12, C). The material has expanded, the expansion being due merely to the elasticity of the substance. Since V_2 is smaller than V_0 , we say the material is imperfectly elastic, $V_2 - V_1$ representing the elastic volume-change and $V_0 - V_2$ the inelastic or permanent volume-change produced by the external pressure.

The elastic expansion from V_1 to V_2 takes place regardless of whether the material is dry or completely immersed; i. e., we will get practically the same result regardless of whether the test is performed on the dry sample or on the same sample completely saturated with and covered by water. Yet, if prior to the removal of the external pressure, all the water standing above the surface of the sample is drained off and the pressure is removed (fig. 12, F), then the material fails to expand. Its volume remains practically unchanged. From the observation made during the first stage of the test (fig. 12, A to C) it is known that it requires a pressure of 1 kilogram per square centimeter to keep the material confined within a space V_1 . As far as the test conditions are concerned, the only difference between the two cases, represented by Figure 12, C, and F, is that in the first case the surface of the sample is completely covered with water while in the second the surface of the sample represents a boundary between air and water. Hence one is compelled to assume that the force which replaced the external pressure, thus preventing the material in the case of Figure 12, F from expanding, resides within the boundary between sample, air and water.

It remains to investigate how that force comes into existence. For this purpose let us consider a vessel simply filled with water. If a steel needle with a somewhat greasy surface is carefully placed on the water surface, the needle floats (fig. 13), whereby it produces a slight depression. Since the specific gravity of the needle is very much greater than the specific gravity of the water, this phenomenon would not be possible unless the water surface behaved like a thin rubber skin with a small, but nevertheless very definite tensile strength. This tensile strength has repeatedly been measured. It amounts to 75 dynes (equal to 0.0764 gram) per centimeter. This value is known as the surface tension of the water.

ACTION OF CAPILLARY PRESSURE ON A COMPRESSIBLE TUBE

The tensile strength of the top layer of the water or the surface tension of the water comes still more into prominence if the lower end of a capillary tube is



FIG. 13.—CAPILLARY FORCE SUPPORTING A GREASY NEEDLE ON WATER SURFACE

dipped into a vessel filled with water. If only a very short piece of the tube sticks out of the water, the water at once shoots up to the upper end of the pipe and stays there. It is obvious that the water could not stay there unless it were held by some force, equal to the weight of the body of water located between the surfaces of the water in the tube and in the vessel. This force is nothing but the tension in the top layer, acting like a rubber skin and tied to the walls of the

tube by molecular attraction. At a constant temperature the surface tension of the water remains always the same (0.0764 gram per centimeter). Since the circumference of the tube is equal to $2\pi r$, the direction of the force acts at an angle α with the vertical and the specific gravity of the water is equal to one, equilibrium requires (fig. 14, A)

$$\pi r^2 y = 0.0764 \times 2\pi r \cos \alpha$$

If the tube is gradually pulled out of the water, the weight of the water to be carried by the surface tension

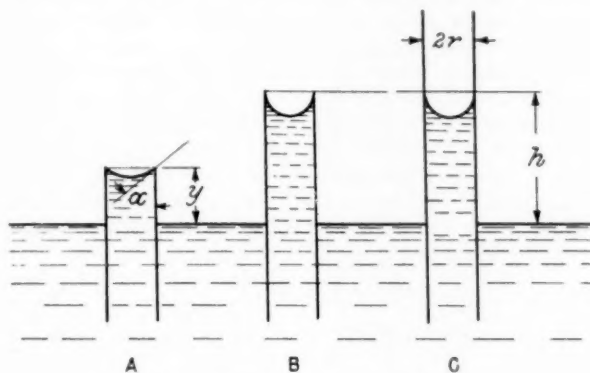


FIG. 14.—WATER IN CAPILLARY TUBES

increases. The surface tension remains the same. Hence, equilibrium requires the value of the angle α to decrease until finally α becomes zero. (Fig. 14, B.) This event marks the maximum height to which the water can possibly rise within the tube. Introducing $y=h$ and $\alpha=0$ into the formula we obtain

$$\pi r^2 h = 0.0764 \times 2\pi r$$

$$\text{or } h = \frac{0.0764 \times 2}{r} = \frac{0.1528}{r} \quad (3)$$

The smaller the radius, r , of the capillary tube the greater is the height, h , to which the water may possibly rise. If the tube is pulled still further out of the water after the height, h , is reached the meniscus (curved water surface within the tube) remains within the tube, at a constant elevation, h , above the outside water level. (Fig. 14, C.)

In order to connect these phenomena with Figure 12, let us consider a capillary tube made out of a very compressible material, such as rubber. At the outset (fig. 15) the tube is supposed to be completely filled with water and the water surfaces at both ends of the tube are practically flat. If the water evaporates, the volume occupied by the water becomes smaller. Yet the same force which drove the water surface up in the tubes (fig. 14) now prevents the water from retiring into the interior of the tubes. (Fig. 15.) Thus, as a result of the evaporation of the water, the surface tension starts to act. The plane water surface of Figure 15, A, passes into a curved one (fig. 15, B) and the axial component of the surface tension produces an equal pressure in the wall of the tube, which in turn causes the compressible wall of the tube to become shorter. This force is equal to $0.0764 \times 2\pi r \cos \alpha$ grams. The more water evaporates, the smaller becomes the angle α . With a decreasing angle α the compressive force increases, until finally, for $\alpha=0$, the force becomes a maximum, corresponding to a maximum shortening of the tube. If, in this or in any

preceding state of the evaporation process the tube is placed under water, the free water surface disappears. With the disappearance of this surface the force acting on the tube disappears, and as a consequence the tube expands, its length increasing again from l_3 to the original value l_1 , provided the tube be perfectly elastic. If the tube is imperfectly elastic, the expansion is smaller than the preceding contraction.

CAPILLARY PRESSURE ON SOILS CALCULATED

The pressure exerted by the surface tension of the water on the wall of the tube may be called the capillary pressure. Capillary pressure fully explains the behavior of the porous sample represented in Figure 12, because it is nothing but a system of compressible capillary tubes whose upper openings are located within the top surface of the sample. By draining the water off the surface of the sample (fig. 12, F) a free water surface is formed within the top surface of the sample, and whereby the pressure of 1 kilogram per square centimeter is still acting. In this state the water surface is still a plane. However, the very moment the pressure is removed the surface tension of the water starts to act. The surface stretching across each individual opening becomes a curve, the angle α assuming such a value that the total force exerted by the capillary pressure becomes equal to the pressure which has been removed, thus keeping the volume of the sample unchanged and equal to V_1 . (Fig. 12, F.)

The replacement of the external pressure by an equal capillary pressure obviously requires that the maximum value of the capillary pressure be equal to or greater than the external pressure which it replaces. Hence it is interesting to figure out how great the force exerted by the capillary pressure may be. For this purpose, suppose we have a sample whose voids have an average width of 0.01 millimeter, which corresponds to the size of voids of a very coarse silt. Assuming the voids are square, every opening would have a perimeter of

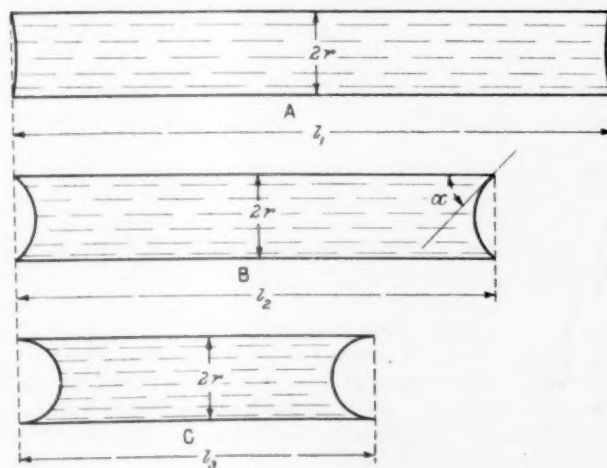


FIG. 15.—SHORTENING OF COMPRESSIBLE TUBES DUE TO CAPILLARY FORCE

0.04 millimeter = 0.004 centimeter, and the force acting on the rim of every opening will be equal to

$$0.004 \times 0.0764 = 0.000306 \text{ grams}$$

This is the force acting on the area of one opening, and as the water extends continuously throughout the whole specimen a force of the same intensity acts over the

entire surface regardless of the actual number of openings per unit of area. The force per square centimeter of surface is therefore the force per opening multiplied by the number of openings per square centimeter, assuming the surface to be completely covered by such openings or

$$\frac{0.000306}{0.001^2} = 306 \text{ grams per square centimeter}$$

In algebraic terms, the computation would be as follows: If the voids of a powder are assumed to be square, the average length of the sides of the square being equal to a in centimeters, the surface tension acting on the rim of each square is equal to

$$4a \times 0.0764 = 0.306a \text{ grams}$$

The area of each opening is equal to a^2 . Hence the maximum value of the capillary pressure will be equal to

$$\frac{0.306a}{a^2} = \frac{0.306}{a} \text{ grams per square centimeter} \dots\dots (4)$$

SOIL SHRINKAGE DUE TO CAPILLARY PRESSURE

From the preceding it is obvious that shrinkage is nothing more than compression produced by a gradual increase of the intensity of the capillary pressure, comparable to the shrinkage of the compressible tube of Figure 15. Swelling represents elastic expansion of the material caused by reducing the capillary pressure to zero. Considering in addition the fact expressed by equation 4, the relation which exists between compressibility, grain size, and volume change due to shrinkage can easily be deduced. For this purpose let us consider a powder or a soil with the compressibility of sample No. 1606 of Figure 1, B. According to this figure, such a soil is approximately as compressible and as elastic as a coarse-grained mixture of 20 per cent mica and 80 per cent sand, because compressibility and elasticity have nothing to do with grain size.

But now, let us take two members of this class, one with an average width of voids of 0.1 mm. and the other with a width of voids of 0.001 mm., mix them with water, so that the water content approximately corresponds to the liquid limit, and then let the water evaporate. As soon as the water starts to evaporate, the surface tension of the water comes into effect, and in both materials the capillary pressure will increase, until it reaches its maximum value. According to equation 4, the maximum value of the capillary pressure will, for the coarse-grained soil, be equal to

$$\frac{0.306}{0.01} = 30.6 \text{ grams per sq. cm.}$$

while for the fine-grained one, it will be as high as

$$\frac{0.306}{0.0001} = 3060 \text{ grams per sq. cm.}$$

To find the volume change produced by these capillary pressures, it is necessary to consult Figure 1. If both materials are assumed to have precisely the same compression curve as sample No. 1606, their initial voids ratio would be 1.56. Under the influence of the capillary pressure, the voids ratio of the coarse-grained material would decrease from 1.56 down to 1.45, corresponding to a volume change of $\frac{1.56 - 1.45}{0.0256} = 4.3$ per cent of the original volume, while the voids

ratio of the finer one would decrease to 0.87, corresponding to a shrinkage of $\frac{1.56 - 0.87}{0.0256} = 27$ per cent of the

original volume. Hence, it is clear that for materials with equal compressibility, the shrinkage increases with decreasing grain size. The shrinkage of the soil shown

in Figure 1, C was found to be equal to $\frac{1.56 - 0.53}{0.0256} =$

40.2 per cent. (0.53 equals shrinkage limit expressed by voids ratio), which indicates that the voids of this material were considerably narrower than 0.001 mm.

On the other hand, for materials with different compressibility but with equal grain size, the maximum values of the capillary pressure will be equal, but the shrinkage will be different. Suppose we have two soils, one of the type of sample No. 1606 of Figure 1, B and one of the friable type like sample No. 1611 of Figure 1, H. If the width of the voids of both materials is equal to 0.001 mm. the maximum value of the capillary pressure will be equal to 3,060 grams per sq. cm. Yet, the volume shrinkage of the soil of

Figure 1, B would be equal to $\frac{1.56 - 0.87}{0.0256} = 27$ per cent

against $\frac{0.626 - 0.485}{0.01626} = 8.68$ per cent for the soil of

Figure 1, H.

The swelling caused by immersing a stiff, plastic or dry piece of soil is determined by the shape of the swelling curves in Figure 1. The steeper these curves, the more intense is the volume change associated with wetting. Hence the shape of the swelling curve serves as an index of the intensity of the swelling of the material.

The action of the surface tension of the water being explained, there remain only two phenomena associated with the shrinking and the swelling of fine-grained soils which can not be traced back to simple capillarity, and which required elaborate investigations before their nature was understood. These two phenomena are the behavior of fine-grained soils upon drying to a water content beyond the shrinkage limit, and the fact that certain fine-grained soils retain part of their cohesion, if they are immersed after having previously been compacted by external or by capillary pressure.

"SOLIDIFIED" WATER BINDS FINE-GRAINED SOILS

If in Figure 15, C, the water continues to evaporate, the meniscus retires into the interior of the tube, the column of water becomes shorter and shorter, and finally, after the water has completely disappeared, the tube has expanded just as completely as if it had been immersed. If we pass from the tube to the powder, one would expect that complete evaporation would cause the powder to expand, and at the same time to lose its cohesion. As a matter of fact, if a very fine-grained sand, having originally some cohesion caused by the presence of water in the voids, is dried, it becomes again perfectly cohesionless. In contrast to this, the cohesion of very fine-grained soils increases upon drying, instead of disappearing. The cause of this phenomenon was found to reside in the fact that water contained in very narrow fissures (smaller than one ten-thousandth of a millimeter) has no longer the physical properties of normal water. It has a higher viscosity, a greater surface tension, and, what seems to be most important of all, it does not evaporate even

if it is heated to the boiling point of normal water.³ Within such openings the water is in what may be called a solidified state. In very fine-grained soils a considerable percentage of the capillary water is confined to openings smaller than the size mentioned above. Hence, when drying the soil at 100° C., the "solidified" part of the water remains and acts similarly to a cement, binding the grains together.

The capacity of certain fine-grained soils to retain part of their cohesion after immersion in water is due to actual cohesion between the soil particles. It has been found that any two bodies, if brought into contact, stick to each other.⁴ The force with which the bodies adhere is so small that under ordinary circumstances it can not be measured. It is even less possible actually to observe it. However, if the number of particles which touch each other is very great, then the adhesion acting at every point of contact becomes evident. Suppose the adhesion per point of contact to be equal to 0.0001 gram. If two pieces of gravel adhere to each other with that force the presence of the force would obviously escape our attention. But if we have an accumulation of soil particles with an average diameter of 0.01 millimeter (size of coarse silt particles), each one of them adhering to its neighbors with a force of 0.0001 gram, the shearing strength of the accumulation would be equal to $1,000^2 \times 0.0001 = 100$ grams per sq. cm. = 0.1 kg. per sq. cm., a shearing strength which involves quite a considerable compressive strength.

CONSISTENCY OF SOILS IN DRY AND SATURATED STATE TO BE DETERMINED

If a fine-grained soil whose original water content was equal to or somewhat above the liquid limit dries out it passes in succession from the liquid through the plastic and the semisolid states into the solid state.⁵ During this process the material becomes stiffer and stiffer, owing to the gradual increase of the intensity of the capillary pressure. We say the material becomes more and more consistent, wherein the term "consistency" indicates the resistance of the material to flow. Methods for determining the consistency have been discussed in a preceding paper.⁶ There remains to consider the states for which the consistency of soils should be determined for the purpose of soil classification.

The extreme states between which the consistency of a subsoil may vary are the dry state and the state of utmost saturation owing to immersion of the soil after a period of drought. The consistency of the soil in the second state seems to have an important bearing on both the bearing capacity of the soil after continued rainfalls and on the slaking properties of the soil. Hence, it was decided to include in the program for final soil tests a compression test on an unconfined, cylindrical sample of the dried soil and a consistency test on a soil sample which has completely expanded, under no pressure, after it has been previously compressed under a pressure of approximately 3.1 kilograms per square centimeter. In order to obtain further information concerning the effect of the type of soil on the consistency in different states, some consistency tests are to be made on soil samples which have

been compressed under a pressure of approximately 3.1 kilograms per square centimeter, without being allowed to expand prior to the test. The consistency tests are simply compression tests performed under standardized conditions on cylindrical, unconfined samples with a diameter of 1 inch.

It is obvious that any change in water content of a soil located at or near the surface of the ground causes the soil to crack. When the soil samples are prepared for consistency tests, the samples have no chance to crack. Hence the results of the consistency tests furnish information only on the consistency of the individual pieces, which, in their totality, would form an "undisturbed" subgrade. Yet, for the purpose of soil classification, such information can be considered sufficient.

CONCLUSIONS

The data on which it is proposed that the final soil classifications be based, give information about the following properties of the subgrade:

1. The volume change produced by a change of the external pressure (load) which acts on the soil (compressibility and elasticity of the soil, represented by compression and swelling curves of the type of Figure 1).
2. The speed with which the volume change follows a change of the pressure (coefficient of consolidation, derived from the results of the time observations by means of equation 2).
3. The permeability of the soil (coefficient of permeability, computed from the coefficient of consolidation or, for more permeable soils, directly obtained by means of a permeability test, performed under standard conditions).
4. Volume change due to drying and wetting, under standard conditions (obtained from the shrinkage limit and from pressure—voids-ratio diagrams of the type of Figure 1).
5. Consistency of the soil in two extreme states.

The technic of the tests required for obtaining the aforementioned data will be described in another paper. All this data has a simple and well-defined bearing on the behavior of the subgrade under load and under variable atmospheric conditions.

The investigations concerning the colloidal character of soil constituents, dye adsorption, base exchange, etc., fall in the same class as the recent investigations concerning the effect of the carbon content, and of various alloys on the strength of steel, or analyses of the physical and chemical action in cement during the process of setting, or similar intricate physicochemical problems relating to construction materials. There is no question of the value of the ultimate results of such investigations. Yet in the classification of construction materials for engineering purposes it is very doubtful whether anything more efficient than the present system, based upon the behavior of the materials under stress, will ever be obtained.

If a road surface cracks because of subsurface conditions, or if a foundation settles, it is due exclusively to a strain in the subgrade, produced by a change of the intensity and distribution of the pressure which acts in the subgrade. Hence, there is no reason to base the final system of soil classification on anything except on the behavior of the soil under various conditions of stress and of confinement. Since the data required for classifying the soils are obtained from actual measurements, performed under standardized conditions, the principles of the system will continue to be valid regardless of the ultimate outcome of physical and chemical investigation of soils.

³ TERZAGHI, CHARLES. VERSUCHE ÜBER DIE VISKOSITÄT DES WASSERS IN SEHR ENGEM DURCHGANGSQUERSCHNITTEN. Zeitschrift für angewandte Mathematik und Mechanik. Band 4, S. 107-113, 1924.

THE MECHANICS OF ADSORPTION AND THE SWELLING OF GELS. Monograph of the Fourth National Colloid Symposium. 1926.

⁴ TERZAGHI, CHARLES. ERDBAUMECHANIK. Pp. 64-66. Vienna, 1925.

⁵ TERZAGHI, CHARLES. SIMPLIFIED SOIL TESTS FOR SUBGRADES AND THEIR PHYSICAL SIGNIFICANCE. PUBLIC ROADS, vol. 7, no. 8, p. 153, Oct., 1926.

⁶ TERZAGHI, CHARLES. DETERMINATION OF THE CONSISTENCY OF SOILS BY PENETRATION TESTS. PUBLIC ROADS, vol. 7, no. 12, Feb., 1927.

ANALYSIS OF STRESSES IN CONCRETE ROADS CAUSED BY VARIATIONS OF TEMPERATURE

By H. M. WESTERGAARD, Associate Professor of Theoretical and Applied Mechanics, University of Illinois

THIS PAPER supplements a previous paper by the writer, published in *PUBLIC ROADS*, April, 1926, under the title "Stresses in concrete pavements computed by theoretical analysis," and in the Proceedings of the Fifth Annual Meeting of the Highway Research Board, held at Washington, D. C., December 3-4, 1925, Part I, 1926, pp. 90-118, under the title "Computation of stresses in concrete roads." Like the previous paper, it rests upon the assumption that the concrete pavement acts as a homogeneous elastic solid, and, as in the former analysis, the method is that of the theory of elasticity, conclusions being drawn from a few simple physical laws by mathematical analysis. In regard to the general assumptions and concepts the reader is referred to the previous paper, which dealt with stresses and deflections produced by wheel loads. The present discussion deals with stresses and deflections produced by variations of temperature. The former paper, on account of the complexity of the mathematical processes involved, was limited to a statement of the assumptions and general principles and to the presentation of the results with illustration of how to use them. Since the mathematical processes involved in the present paper are much simpler, it was considered to be expedient not to omit them. Results are given in tables and diagrams, and the use of the results is illustrated by numerical examples.

The fact that cracks sometimes develop in a new pavement before any load is put on it shows the importance of the stresses which ordinarily are considered to be secondary—stresses caused by changes of temperature, by setting of the concrete, and by changes of moisture content. In a piece of concrete free to expand and contract the setting will produce a shrinkage equal to that caused by a certain drop in temperature, and the absorption of moisture will produce a swelling equal to that produced by a certain rise in temperature. In each case the essential feature is a tendency to change of volume. Thus, the study of stresses due to variations of temperature will supply information also about the other secondary stresses. With this condition in view, the discussion is limited to the case of variations of temperature.

The stresses caused by variations of temperature should be considered from two points of view. One has reference to the early life of the pavement, before the pavement has obtained its full strength and before it has been opened to traffic. The other has reference to the later life, after the pavement has gained strength and after it has been opened to traffic. According to the first point of view, the stresses caused by variations of temperature are considered as an independent cause of cracks and are treated by themselves. According to the other point of view, the temperature stresses are to be combined with the stresses caused by the loads. This combination, in most cases, is a simple matter of addition.

Whatever particular effect is studied, three places on the panel of pavement should be examined—the corners, the interior area, and the edges.

Two major cases will be investigated. The first arises from a consideration of the slow seasonal changes of temperature; the second from a consideration of quick changes of temperature, occurring, for example, by the change from a cool night to a hot day, and vice versa. In the first case the final temperature is assumed to be uniform throughout the thickness of the pavement. The second case is dealt with by assuming a definite temperature gradient through the thickness of the pavement with the temperature unchanged at the middle plane. The stresses in this case are dependent upon the manner in which the slab deflects or curls. Obviously, the stresses found in these two major cases may have to be combined by addition or subtraction.

STRESSES CAUSED BY UNIFORM DECREASE OF TEMPERATURE

Let it be assumed that the temperature has decreased the same amount all through the depth of the pavement. What, then, is the effect upon the pavement?

In order to explain the analysis which follows it will be desirable to describe in general terms the behavior of the panel or slab of concrete when its temperature decreases uniformly. The immediate result is that there is a tendency for the slab to contract both longitudinally and transversely. The contraction is resisted by friction between the slab and the subgrade and as a result tensile stresses, both longitudinal and transverse, are set up in the concrete. These stresses tend to elongate the slab in the two directions in which they act and to shorten it in the direction at right angles to their line of action. The longitudinal tensile stress induces a longitudinal elongation and a transverse shortening. This transverse shortening bears to the longitudinal elongation the relation defined by Poisson's ratio, μ . The transverse tensile stress induces a transverse elongation and a longitudinal shortening. The ratio of this shortening, per unit of length, to the elongation, per unit of length, is Poisson's ratio, μ .

Consider, then, the action which takes place in the longitudinal direction: The slab contracts as a result of the decreased temperature; the contraction is resisted by the friction offered by the subgrade, and the longitudinal tensile stress thus set up causes an elongation which diminishes the amount of contraction that would otherwise occur; but the transverse tensile stress, which is set up in the same way by friction in the transverse direction, again increases the longitudinal contraction; so that the net result is a combination of three tendencies.

The elongations per unit of length resulting are expressed by the following equations:

$$\epsilon_x = \frac{1}{E}(\sigma_x - \mu\sigma_y) - \epsilon_t, \quad \epsilon_y = \frac{1}{E}(\sigma_y - \mu\sigma_x) - \epsilon_t \quad (1)$$

in which x, y = horizontal rectangular coordinates
 σ_x, σ_y = normal tensile stresses in the directions of x or y , respectively,
 ϵ_x, ϵ_y = elongations per unit of length in the directions of x or y , respectively,
 E = modulus of elasticity of concrete,
 μ = Poisson's ratio for the concrete,
 ϵ_t = coefficient of temperature expansion,
 t = decrease of temperature.

At a corner of an unloaded panel of pavement, obviously, there can be no stresses σ_x and σ_y . At a small distance from the corner, stresses may develop if the friction offered by the subgrade is considerable. In that case the loads are the least likely to produce a corner break, because the existence of considerable subgrade friction would imply a strong subgrade support. The uniform drop of temperature, therefore, is not likely to be important as a contributory cause of a corner break.

Consider next the central area of a large panel. Assume that the friction is sufficient to prevent the slab from contracting in either direction, i. e., to make $\epsilon_x = 0$ and $\epsilon_y = 0$. Then by solving the two equations 1, one finds

$$\sigma_x = \sigma_y = \frac{E\epsilon_t t}{1-\mu} \quad (2)$$

Consider finally an edge of the panel, parallel to the axis of x . Consider a point of this edge at an appreciable distance from any corner, and assume the friction to be sufficient to make $\epsilon_x = 0$. Obviously there can be no stress perpendicular to the edge at the edge. With $\sigma_y = 0$ one finds by equations 1, at the edge,

$$\sigma_x = E\epsilon_t t \quad (3)$$

The stresses given by equations 2 and 3 may have to be added to those caused by the loads.¹

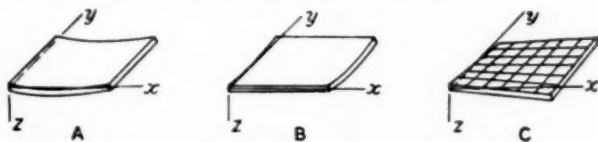


FIG. 1.—DEFORMATIONS OF ELEMENT OF SLAB

In a numerical example assume $E = 3,000,000$ pounds per square inch, $\mu = 0.15$, $\epsilon_t = 0.0000060$ per degree Fahrenheit, and $t = 50^\circ$ F. Then equations 2 and 3 give $\sigma_x = \sigma_y = 1,059$ pounds per square inch in the central area, and $\sigma_x = 900$ pounds per square inch at the edge. One may note that a shrinkage of 0.0003 inch per inch, an entirely possible value, would produce the same stresses, which, it will be noted, are those that would be developed if the concrete were capable of withstanding without shrinkage or cracking a drop in temperature of 50° F.

The possibility exists both in the case of low temperature in the cold season and in the case of shrinkage that a plastic flow of the concrete may relieve these stresses appreciably. Otherwise the large stresses computed can be relieved only by the presence of joints or the forming of cracks, combined with a sufficient amount of sliding of the pavement on the subgrade.²

CURLING STRESSES AND DEFLECTIONS

Assume next that the temperature remains normal at the middle plane of the pavement, but is t degrees lower at the top of the pavement than at the bottom.

¹ WESTERGAARD, H. M. STRESSES IN CONCRETE PAVEMENTS COMPUTED BY THEORETICAL ANALYSIS. PUBLIC ROADS, April, 1926 [or COMPUTATION OF STRESSES IN CONCRETE ROADS. Proceedings of the fifth annual meeting of the Highway Research Board, December 3-4, 1925, Pt. I, p. 90, 1926]. Tables 3 and 4 in this paper contain values of the stresses produced by a wheel load of 10,000 pounds in the central area and at the edge, respectively.

² For a discussion of the spacing of joints required to prevent cracking, see GOLDBECK, A. T., THE INTERRELATION OF LONGITUDINAL STEEL AND TRANSVERSE CRACKS IN CONCRETE ROADS. PUBLIC ROADS, vol. 6, No. 6, August, 1925.

Assume a uniform temperature gradient through the thickness, h , of the slab. Assume that the reactions of the subgrade are vertical only, and equal to kz per unit of area, where z is the deflection (positive downward) and k is a constant "modulus of subgrade reaction."³

Under the assumed temperature condition—i. e., the temperature lower at the top than at the bottom—the slab will tend to curl upward at the edge, and its state of flexure may be resolved into three component parts as follows: Bending in the x -direction (fig. 1, A), bending in the y -direction (fig. 1, B), and torsion or twisting in the xy -directions (fig. 1, C). The amounts of the deformations are measured in Figures 1, A and

B, by the curvatures $-\frac{\partial^2 z}{\partial x^2}$ and $-\frac{\partial^2 z}{\partial y^2}$ (as in beams), and in Figure 1, C, by the rate of change of slope; that is, by $-\frac{\partial^2 z}{\partial x \partial y}$.

If now, we denote by M_x and M_y the bending moments in the directions of x and y , respectively, per unit of width of cross section, and by M_z the twisting moment in the directions of x and y per unit of width of cross section,⁴ then the curvatures of the elastic surface (the bent middle plane) in the directions of x and y , respectively, will be:

$$\left. \begin{aligned} -\frac{\partial^2 z}{\partial x^2} &= \frac{12}{Eh^3}(M_x - \mu M_y) + \frac{\epsilon_t t}{h}, \\ -\frac{\partial^2 z}{\partial y^2} &= \frac{12}{Eh^3}(M_y - \mu M_x) + \frac{\epsilon_t t}{h}, \end{aligned} \right\} \quad (4)$$

and the twist in the directions of x and y will be:

$$-\frac{\partial^2 z}{\partial x \partial y} = \frac{12(1+\mu)}{Eh^3} M_z \quad (5)$$

The thickness, h , and the difference of temperature, t , will be assumed from here on to be the same at all points of the slab.

Center stress of a broad and long slab.—Consider first the central area of a long and broad unloaded panel. At a sufficient distance from the edges the deflections, z , must be zero, i. e., the curvatures of the slab must be zero. Then the equations just stated give

$$M_x = M_y = -\frac{Eh^2 \epsilon_t t}{12(1-\mu)}, \quad M_z = 0 \quad (6)$$

The corresponding tensile stress at the top is found by dividing $-M_x$ by the section modulus per unit of width, $\frac{h^2}{6}$; and this tensile stress, which is the same in all horizontal directions, is

$$\sigma_o = \frac{E\epsilon_t t}{2(1-\mu)} \quad (7)$$

By substitution, then, with $E = 3,000,000$ pounds per square inch, $\mu = 0.15$, and $\epsilon_t = 0.0000060$ per degree Fahrenheit, as before, and $t = 10^\circ$ F., one finds the

³ A discussion of the assumptions involved here, especially in regard to the reactions of the subgrade, may be found in the paper entitled, "Stresses in concrete pavements computed by theoretical analysis," PUBLIC ROADS, April, 1926.

⁴ Concerning the character and action of these moments, see WESTERGAARD, H. M., and SLATER, W. A., MOMENTS AND STRESSES IN SLABS, Proc. Am. Concrete Inst. v. 17, 1921, p. 415, especially, p. 424, or, Nat. Research Council, Reprint and Circular Series, No. 32, especially p. 10.

stress at the top to be $\sigma_o = 106$ pounds per square inch.

This, it may be well to repeat, is the stress which would be caused by a difference of temperature of 10° in the central area of a broad and long slab, where, by reason of the distance from the edge, there is no deflection.

With $t = -10^\circ \text{ F.}$, that is, with the temperature 10° higher at the top than at the bottom, the same tensile stress will be found at the bottom of the pavement, and, in this case, may have to be added to the stress produced by wheel loads.⁵

Deflection and stress at points near the edge of a broad and long slab.—Consider next a slab which has an edge along the axis of x , and which extends infinitely far in the directions of positive and negative x and positive y . With the difference of temperature between top and bottom the same all over the slab, the deflection, z , is a function of y only, independent of x .

One finds, then, by eliminating M_x in equations 4:

$$M_y = \frac{Eh^3}{12(1-\mu^2)} \left(-\frac{d^2z}{dy^2} - \frac{(1+\mu)\epsilon t}{h} \right) \quad (8)$$

The reactions of the subgrade, kz , are the only external forces to be taken into consideration. The expression kz may be applied when z is negative (upward) provided that there is still contact between the slab and the subgrade. This contact may be maintained by the weight of the pavement or by this weight in conjunction with loads the effects of which are to be added afterwards to the effects of the variation of temperature.

The equilibrium of any small element of the slab requires, accordingly,

$$\frac{d^2M_y}{dy^2} = kz \quad (9)$$

By substituting M_y from equation 8 one finds:

$$\frac{Eh^3}{12(1-\mu^2)} \frac{d^4z}{dy^4} + kz = 0 \quad (10)$$

Here, as in other investigations of slabs on elastic subgrade, it is expedient to introduce the linear distance,

$$l = \sqrt[4]{\frac{Eh^3}{12(1-\mu^2)k}} \quad (11)$$

which is called the "radius of relative stiffness." This distance is a measure of the stiffness of the slab relative to the stiffness of the subgrade. Table 1 gives values of the radius of relative stiffness for different values of h and k .⁶

⁵ See Table 3 in the paper, "Stresses in concrete pavements computed by theoretical analysis."
⁶ Table 1 is the same as Table 1 in the paper, "Stresses in concrete pavements computed by theoretical analysis."

TABLE 1.—Values of the radius of relative stiffness, l , for different values of the slab thickness, h , and of the modulus of subgrade reaction, k , computed from equation 11

[$E=3,000,000$ pounds per square inch, $\mu=0.15$]

Thickness of slab in inches h	Radius of relative stiffness, l , in inches		
	$k=50 \text{ lb./in.}^2$	$k=100 \text{ lb./in.}^2$	$k=200 \text{ lb./in.}^2$
4.....	23.91	20.11	16.92
5.....	28.28	23.78	20.00
6.....	32.40	27.26	22.92
7.....	36.40	30.60	25.73
8.....	40.23	33.83	28.44
9.....	43.94	36.95	31.07
10.....	47.55	40.00	33.62
11.....	51.08	42.94	36.11
12.....	54.52	45.84	38.56

With l introduced, equation (10) becomes:

$$l^4 \frac{d^4z}{dy^4} + z = 0 \quad (12)$$

In the present case the functions z and $\frac{dz}{dy}$ must converge toward zero when y increases indefinitely. Furthermore, at the edge, $y=0$, the bending moment, M_y , and the vertical shear, $\frac{dM_y}{dy}$, must also be zero. The following solution is correct because it satisfies these end conditions as well as equation 12:

$$z = -z_o \sqrt{2} \cos \left(\frac{y}{l\sqrt{2}} + \frac{\pi}{4} \right) e^{-\frac{y}{l\sqrt{2}}} \quad (13)$$

where e is the base of the Napierian system of logarithms and

$$z_o = \frac{(1+\mu)\epsilon t l^2}{h} = \epsilon t \sqrt{\frac{(1+\mu)Eh}{12(1-\mu)k}} \quad (14)$$

is the reversed (upward) deflection at the edge, $y=0$.

By substituting these expressions in equation (8) one finds the bending moment M_y . By dividing $-M_y$ by the section modulus per unit of width, $\frac{h^2}{6}$, the result is the tensile stress at the top of the slab in the direction of y ,

$$\sigma_y = \sigma_o \left(1 - \sqrt{2} \sin \left(\frac{y}{l\sqrt{2}} + \frac{\pi}{4} \right) e^{-\frac{y}{l\sqrt{2}}} \right) \quad (15)$$

where

$$\sigma_o = \frac{E\epsilon t}{2(1-\mu)}$$

(same as equation 7)

By solving the first of equations 4 for M_x with $\frac{d^2z}{dx^2} = 0$, and dividing $-M_x$ by the section modulus, $\frac{h^2}{6}$

one finds the tensile stress at the top, in the direction of x ,

$$\sigma_x = \frac{E\epsilon_t t}{2} + \mu\sigma_y = \sigma_o + \mu(\sigma_y - \sigma_o), \quad (16)$$

or, by substituting σ_y from equation 15,

$$\sigma_x = \sigma_o \left(1 - \mu\sqrt{2} \sin \left(\frac{y}{l\sqrt{2}} + \frac{\pi}{4} \right) e^{-\frac{y}{l\sqrt{2}}} \right), \quad (17)$$

These expressions for z , σ_y and σ_x (equations 13, 15, and 17) all apply to the condition of a slab of infinite extent in the directions of x and y . The function, z , is the deflection in the transverse direction occurring at

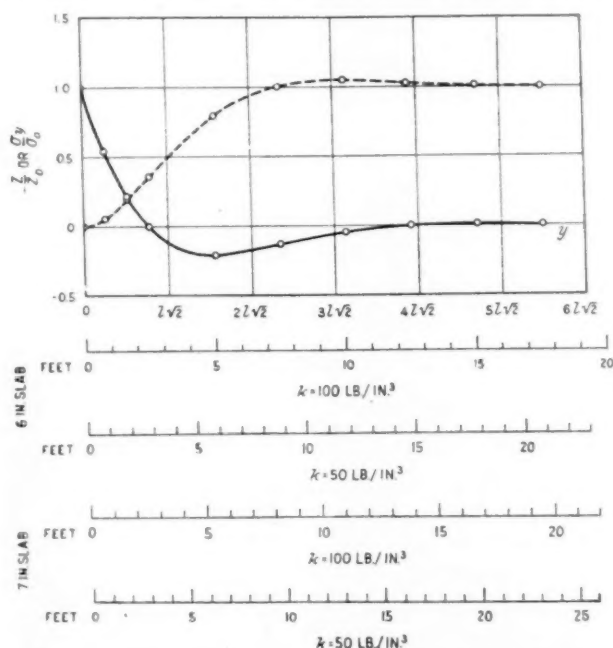


FIG. 2.—THE CURLING OF A PAVEMENT WHEN THE TEMPERATURE IS NORMAL AT THE MIDDLE PLANE, AND t DEGREES LOWER AT THE TOP THAN AT THE BOTTOM. THE PAVEMENT, INFINITELY WIDE IN THE DIRECTION OF y , COVERS THE WHOLE POSITIVE SIDE OF THE AXIS OF x . THE HORIZONTAL DISTANCES, y , ARE MEASURED FROM THE EDGE. THE ORDINATES OF THE FULL-LINE CURVE REPRESENT RELATIVE VALUES OF THE DEFLECTIONS, z , AND THOSE OF THE DOTTED CURVE REPRESENT RELATIVE VALUES OF THE TENSILE STRESSES, σ_y , AT THE TOP OF THE PAVEMENT IN THE DIRECTION PERPENDICULAR TO THE EDGES. SCALES FOR y ARE GIVEN IN TERMS OF l FOR GENERAL APPLICATION, AND NUMERICALLY IN FEET FOR SLAB THICKNESSES OF 6 AND 7 INCHES AND VALUES OF k EQUAL TO 50 AND 100 POUNDS PER CUBIC INCH FOR EACH SLAB THICKNESS

any distance, y , from the edge of the slab and it is expressed in equation (13) in terms of z_o , the deflection of the edge. The stresses σ_x and σ_y are principal stresses, one the greatest, the other the smallest at the particular point, and both are expressed (equations 15 and 17) in terms of the stress, σ_o , corresponding to points in the central area of the slab at which, by reason of distance from the edge there is no deflection. There are no shearing stresses in the directions of x and y .

Although this case is not similar to that of any ordinary pavement condition, since pavement widths

are relatively narrow, the relative values of z in terms of z_o and of σ_y in terms of σ_o are shown by the full and dotted curves, respectively, in Figure 2. The general scale, giving distances from the edge in terms of l , is converted into feet for thicknesses of 6 and 7 inches and for values of k equal to 100 and 50 pounds per cubic inch, in accordance with the values given in Table 2. The same table gives also the corresponding values of the edge deflection, z_o , the stress σ_o being for all thicknesses and values of k the same and equal to 106 pounds per square inch (see example under equation 7). By reference to the scales in feet it will be observed that the stress of 106 pounds per square inch and zero deflection obtain at all points more distant than 18 feet from the edge in a 6-inch slab with a modulus of subgrade reaction equal to 100 and varying from this distance to 24 feet for the 7-inch slab with a subgrade modulus of 50.

TABLE 2.—Examples of values of the reversed deflection, z_o , at the edge in the case of Figure 2, computed from equation 14, for $E=3,000,000$ pounds per square inch, $\mu=0.15$

[$\epsilon_t=0.000060$ per degree Fahrenheit, $t=10^\circ$ F. for typical values of the thickness of the slab, h , and the modulus of subgrade reaction, k . Corresponding value of the stress σ_o according to equation (7): $\sigma_o=106$ pounds per square inch. The values of l are taken from Table 1]

h inches	k lb./in. ³	l inches	z_o inches
6	100	27.26	0.0085
6	50	32.40	.0121
7	100	30.60	.0092
7	50	36.40	.0131

The case of a long slab of relatively narrow width.—The next case to consider is that of an infinitely long strip or slab of finite width b . Let the center line be along the axis of x . Then the edges have the equations, $y = \pm \frac{b}{2}$. This case corresponds approximately to that of a newly constructed pavement not yet cracked transversely, in which the unjointed length is great in comparison with the width.

Assume again the difference of temperature between the top and the bottom of the slab to be constant and equal to t . Then, as in the previous case, the deflection, z , will be a function of y only, independent of x . The flexure will be governed again by equations 8, 9, 10, 12, and 16. The end conditions in this case are: $M_y = 0$, $\frac{dM_y}{dx} = 0$, at the edges $y = \pm \frac{b}{2}$. The following solution is correct because it satisfies these end conditions and the differential equation 12:⁷

$$z = -z_o \frac{2 \cos \lambda \cos h\lambda}{\sin 2\lambda + \sin h2\lambda} \left[(-\tan \lambda + \tan h\lambda) \cos \frac{y}{l\sqrt{2}} \cos h \frac{y}{l\sqrt{2}} + (\tan \lambda + \tan h\lambda) \sin \frac{y}{l\sqrt{2}} \sin h \frac{y}{l\sqrt{2}} \right] \quad (18)$$

where

$$\lambda = \frac{b}{l\sqrt{8}} \quad (19)$$

and, as before,

$$z_o = \frac{(1+\mu)\epsilon_t t}{h} l^2 = \epsilon_t t \sqrt{\frac{(1+\mu)Eh}{12(1-\mu)k}} \quad (\text{same as equation 14})$$

⁷ Equations 13 and 18 and corresponding expressions for M_x and M_y were stated in a paper by the writer, OM BEREKNING AF FLADER PAA ELASTISK UNDERLAG MED SAERLIGT HENBLIK PAA SPØRGSMÅLET OM SPAENDINGER I BETONVEJE. Ingeniøren, v. 32, p. 513, 1923, Copenhagen. See p. 524.

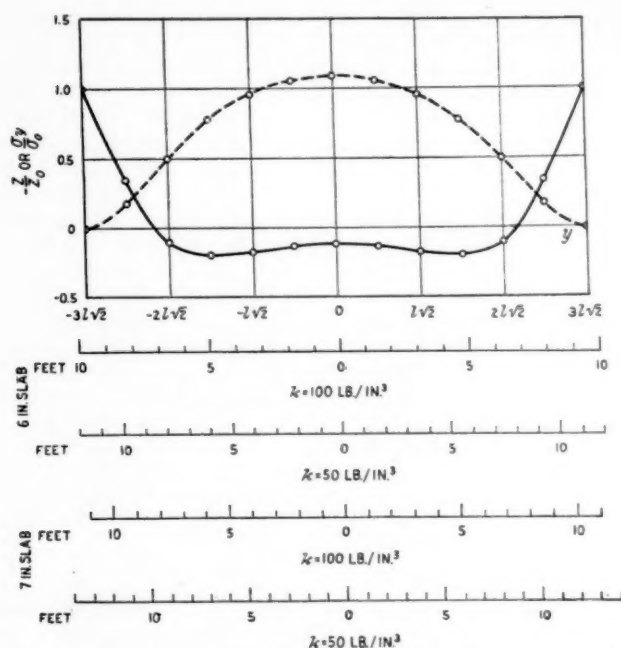


FIG. 3.—THE CURLING OF A PAVEMENT OF WIDTH $b=6l\sqrt{2}$ WHEN THE TEMPERATURE IS NORMAL AT THE MIDDLE PLANE, AND t DEGREES LOWER AT THE TOP THAN AT THE BOTTOM. THE HORIZONTAL DISTANCES, y , ARE MEASURED FROM THE CENTER LINE OF A STRIP OF PAVEMENT INCLOSED BETWEEN THE LINES $y=\pm\frac{b}{2}$. THE ORDINATES OF THE FULL-LINE CURVE REPRESENT RELATIVE VALUES OF THE DEFLECTIONS, z , AND THOSE OF THE DOTTED CURVE REPRESENT RELATIVE VALUES OF THE TENSILE STRESSES, σ_y , AT THE TOP OF THE PAVEMENT IN THE DIRECTION PERPENDICULAR TO THE EDGES. SCALES FOR y ARE GIVEN IN TERMS OF l FOR GENERAL APPLICATION, AND NUMERICALLY IN FEET FOR SLAB THICKNESSES OF 6 AND 7 INCHES AND VALUES OF k EQUAL TO 50 AND 100 POUNDS PER CUBIC INCH FOR EACH SLAB THICKNESS

By the process applied in the preceding case one finds the corresponding principal stresses at the top of the slab:

$$\sigma_y = \sigma_o \left[1 - \frac{2 \cos \lambda \cos h\lambda}{\sin 2\lambda + \sin h2\lambda} \left((\tan \lambda + \tan h\lambda) \cos \frac{y}{l\sqrt{2}} \cos h \frac{y}{l\sqrt{2}} + (\tan \lambda - \tan h\lambda) \sin \frac{y}{l\sqrt{2}} \sin h \frac{y}{l\sqrt{2}} \right) \right] \quad (20)$$

$$\sigma_x = \sigma_o + \mu (\sigma_y - \sigma_o) \quad (21)$$

where, as before,

$$\sigma_o = \frac{E\epsilon_1 t}{2(1-\mu)} \quad (\text{same as equation 7})$$

Numerical computations by equations 18 and 20 become a simple matter by use of a book of tables published by Hayashi in 1921.⁸ These tables give the values of the hyperbolic and natural sines and cosines in a convenient form, and they have been used in making the computations given in Tables 3 and 4 and graphically in Figures 2, 3, 4, and 5.

Table 3 and Figures 3 and 4 show the relative deflections and stresses at different distances from the center line of a pavement of two different widths, one half as great as the other. Deflections are expressed as functions of the edge deflection of a slab of infinite width, and the stresses are expressed in terms of σ_o , the stress in

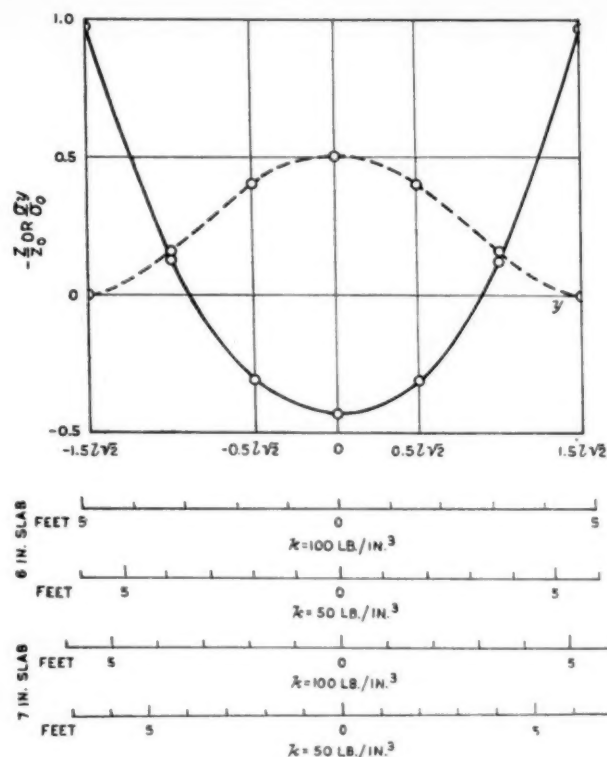


FIG. 4.—THE CURLING OF A PAVEMENT OF WIDTH $b=3l\sqrt{2}$ (ONE-HALF THE WIDTH OF THE PAVEMENT REPRESENTED BY FIGURE 3), WHEN THE TEMPERATURE IS NORMAL AT THE MIDDLE PLANE, AND t DEGREES LOWER AT THE TOP THAN AT THE BOTTOM. THE HORIZONTAL DISTANCES, y , ARE MEASURED FROM THE CENTER LINE OF THE STRIP OF PAVEMENT INCLOSED BETWEEN THE LINES $y=\pm\frac{b}{2}$. THE ORDINATES OF THE FULL-LINE CURVE REPRESENT RELATIVE VALUES OF THE DEFLECTIONS, z , AND THOSE OF THE DOTTED CURVE REPRESENT RELATIVE VALUES OF THE TENSILE STRESSES, σ_y , AT THE TOP OF THE PAVEMENT IN THE DIRECTION PERPENDICULAR TO THE EDGES. SCALES FOR y ARE GIVEN IN TERMS OF l FOR GENERAL APPLICATION, AND NUMERICALLY IN FEET FOR SLAB THICKNESSES OF 6 AND 7 INCHES AND VALUES OF k EQUAL TO 50 AND 100 POUNDS PER CUBIC INCH FOR EACH SLAB THICKNESS

the central portion of such an infinite slab. By comparison of the two figures and the columns of the table corresponding to the two widths one sees clearly the effect upon deflections and stresses of cutting the continuous width of a pavement slab in half by the introduction of a center joint. By so doing, for example, it appears that the edge deflections are not appreciably altered, but the maximum stress is reduced by more than half.

According to the numerical scales at the bottom of Figures 3 and 4, the diagram (fig. 3) may represent, for example, a pavement 20 feet wide without center joint and still uncracked. The maximum stress, σ_y , at the center (see also Table 3) is $1.084\sigma_o$. If this pavement cracks along the center line, the left half of it will be represented by the diagram (fig. 4), and, as will be seen, the maximum value of σ_y becomes $0.508\sigma_o$. With $\mu=0.15$ the corresponding stresses, σ_x , in the direction of the road become, according to equation 21:

In the case represented by Figure 3,

$$\sigma_x = \sigma_o (1 + 0.15 \times 0.084) = 1.013\sigma_o$$

⁸ HAYASHI, K. FÜNFSTELLIGE TAFELN DER KREIS- UND HYPERBELFUNKTIONEN SOWIE DER FUNKTIONEN e^x UND e^{-x} MIT DEN NATÜRLICHEN ZAHLEN ALS ARGUMENT. Berlin and Leipzig, 1921. (Walter de Gruyter & Co.)

and in the case represented by Figure 4,

$$\sigma_x = \sigma_o (1 - 0.15 \times 0.492) = 0.926 \sigma_o.$$

That is, in order that the stress σ_x shall be relieved in a manner comparable to that of σ_y , transverse cracks or joints are required. At the edge, without transverse cracks or joints, the stresses are the same before and after the longitudinal crack has formed, being, respectively,

$$\sigma_y = 0 \text{ and } \sigma_x = 0.85 \sigma_o.$$

TABLE 3.—Two examples of curling of a strip of pavement of width b , when the temperature at the top of the pavement is t degrees lower than at the bottom

Relative values of the deflections, z , and the stresses, σ , across the strip, at different distances, y , from the center line, from equations 18 and 20. Graphical representation in Figures 3 and 4. Examples of numerical values of z_o and σ_o are given in Table 2]

$\frac{y}{l\sqrt{2}}$	$b=6l\sqrt{2}$		$b=3l\sqrt{2}$	
	$\frac{z}{z_o}$	$\frac{\sigma}{\sigma_o}$	$\frac{z}{z_o}$	$\frac{\sigma}{\sigma_o}$
0	0.1126	1.084	0.4320	0.508
0.5	.1326	1.056	.3049	.405
1	.1773	.959	-.1260	.163
1.5	.1980	.775	-.9720	.000
2	.1021	.493		
2.5	-.3476	.178		
3	-1.003	.000		

TABLE 4.—Curling of a strip of pavement of width b , when the temperature at the top of the pavement is t degrees lower than at the bottom

[Relative values of the deflections, z_o , at the edge, and of the stresses, σ_o , across the center line, for different values of b , computed from equations 18 with $y=\frac{b}{2}$, and 20 with $y=0$. Graphical representation in Figure 5. Examples of numerical values of z_o and σ_o are given in Table 2]

$\frac{b}{l\sqrt{8}} (= \lambda)$	$\frac{b}{l}$	$\frac{z_o}{z_o}$	$\frac{\sigma_o}{\sigma_o}$
∞	∞	-1.000	1.000
4	11.31	-0.999	1.052
3	8.49	-1.003	1.084
2.5	7.07	-1.026	1.032
2.365	6.69	-1.036	1.000
2	5.66	-1.057	0.856
1.571	4.44	-1.000	
1.5	4.24	-0.972	0.508
1	2.828	-0.599	0.148
0.5	1.414	-0.165	0.010

TABLE 5.—Example of stresses, in pounds per square inch, occurring in a 20-foot pavement without transverse cracks or joints, before and after a longitudinal crack has formed along the center line

The temperature at the top of the pavement is assumed to be 10° F. lower than at the bottom. $E=3,000,000$ pounds per square inch; $\mu=0.15$; $\epsilon_t=0.0000060$ per degree Fahrenheit; $\sigma_o=106$ pounds per square inch (compare Table 2)]

	Before cracking longitudinally		After cracking longitudinally	
	Center of 20-foot strip	Edge	Center of 10-foot strip	Edge
Transverse stress, σ_y (pounds per square inch)	115	0	54	0
Longitudinal stress, σ_x (pounds per square inch)	107	90	97	90

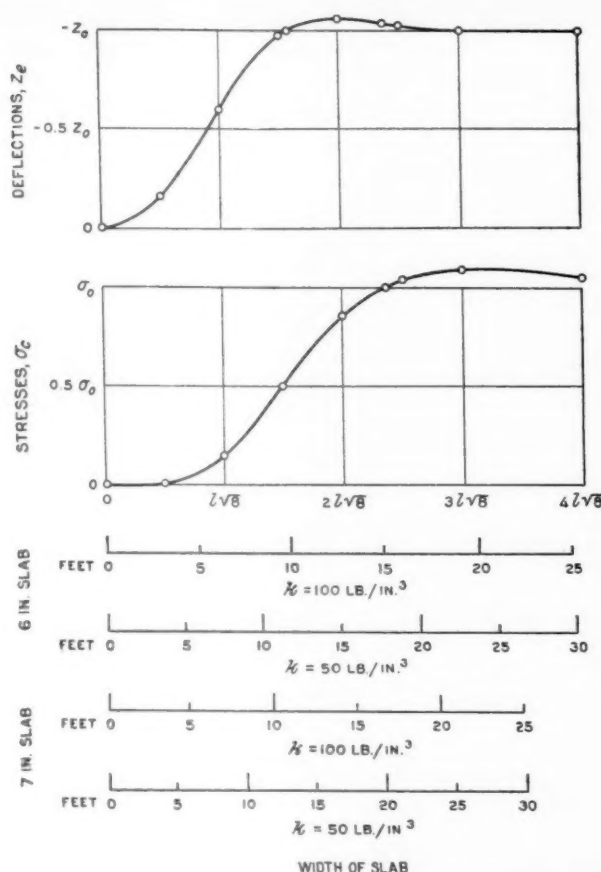


FIG. 5.—CURLING OF A STRIP OF PAVEMENT OF WIDTH b , WHEN THE TEMPERATURE IS NORMAL AT THE MIDDLE PLANE, AND t DEGREES LOWER AT THE TOP THAN AT THE BOTTOM, GIVING VALUES OF THE DEFLECTIONS, z_e , AT THE EDGE, AND THE STRESSES, σ_o , ACROSS THE CENTER LINE, FOR DIFFERENT VALUES OF b . THE SCALES FOR b AT THE BOTTOM OF THE FIGURE APPLY FOR THE PARTICULAR VALUES OF h AND k STATED IN TABLE 2

Table 5 shows numerical values obtained by this procedure on the basis of the values assumed in connection with Table 2. Stresses like those in Table 5 may have to be combined with the stresses resulting from a superimposed uniform drop of temperature (drop of temperature in the middle plane of the slab), with forces of friction active between the slab and the subgrade.

By assuming $t = -10^\circ$ F. instead of $+10$ degrees—that is, by assuming the top of the pavement to be 10 degrees warmer than the bottom, the tensile stresses given in Table 5 will still exist, but will be at the bottom of the pavement instead of at the top. These tensions at the bottom are significant in that they may have to be combined with the tensions due to wheel loads, both in the central area and at the edge.⁹

Edge deflections and center stresses tabulated for purposes of practical design.—In Table 4 and Figure 5 are given the relative edge deflections and center stresses in slabs of various widths corresponding to the several

⁹ Values of these stresses due to wheel loads are given in Tables 3 and 4 in the paper "Stresses in concrete pavements computed by theoretical analysis."

values of b . Here again the deflections and stresses are given in terms of the edge deflection and interior stress, respectively, of a slab of infinite width, and the values given for both are maxima for the several widths represented.

Since these factors, i. e., the edge deflection and the center stress for slabs of finite width, are of greatest practical importance for purposes of design, Tables 6 and 7 have been compiled to show the numerical values of the two factors for a range of thickness and width of slab embracing the common dimensions and for three values of the modulus of subgrade reaction, k . The values given in these tables are based on a difference of temperature of 10° F. between the top and bottom of the slab. Values corresponding to any other difference of temperature may be obtained by multiplying the tabulated values by $\frac{t}{10}$, where t represents the difference of temperature assumed for purposes of design.

TABLE 6.—Edge deflections of concrete slabs of infinite length¹ and various widths and thicknesses, corresponding to three values of the modulus of subgrade reaction, when the difference of temperature between the top and bottom of the slab is 10° F.

[$E=3,000,000$ pounds per square inch, $\mu=0.15$, $\epsilon_1=0.0000060$]

Modulus of subgrade reaction k	Thickness of slab in inches	Width of slab in feet							
		9	12	14	16	18	20	24	30
		Edge deflection in inches							
50-----	6	0.0092	0.0121	0.0127	0.0127	0.0125	0.0123	0.0121	0.0121
	7	.0085	.0121	.0133	.0138	.0138	.0136	.0132	.0130
	8	.0077	.0116	.0134	.0144	.0148	.0147	.0143	.0140
100-----	10	.0062	.0104	.0128	.0146	.0158	.0164	.0164	.0158
	6	.0079	.0090	.0090	.0088	.0086	.0086	.0085	.0086
	7	.0076	.0095	.0098	.0097	.0095	.0093	.0092	.0092
200-----	8	.0071	.0096	.0103	.0104	.0103	.0101	.0099	.0099
	10	.0061	.0093	.0107	.0114	.0117	.0116	.0113	.0110
	6	.0062	.0063	.0062	.0061	.0060	.0060	.0060	.0060
	7	.0063	.0069	.0068	.0066	.0066	.0065	.0065	.0065
	8	.0062	.0073	.0074	.0072	.0071	.0070	.0070	.0070
	10	.0056	.0076	.0082	.0082	.0081	.0080	.0078	.0078

¹ For practical purposes the values given in the table apply also to slabs the length of which with respect to the width is relatively great.

TABLE 7.—Stresses across the center line of concrete slabs of infinite length¹ and various widths and thicknesses, corresponding to three values of the modulus of subgrade reaction, when the difference of temperature between the top and bottom of the slab is 10° F.

[$E=3,000,000$ pounds per square inch, $\mu=0.15$, $\epsilon_1=0.0000060$]

Modulus of subgrade reaction k	Thickness of slab in inches	Width of slab in feet							
		9	12	14	16	18	20	24	30
		Center stress in pounds per square inch							
50-----	6	27	60	80	96	106	112	115	112
	7	18	45	65	82	96	105	114	114
	8	13	34	52	70	85	96	110	115
100-----	10	10	20	33	48	63	77	98	112
	6	45	83	99	109	114	115	113	104
	7	33	68	87	101	109	113	115	110
200-----	8	24	54	75	91	102	110	115	113
	10	13	35	53	70	85	97	110	115
	6	68	101	111	115	115	113	109	106
	7	53	90	104	112	115	115	112	107
	8	40	77	95	107	112	115	114	109
	10	24	55	75	92	103	110	115	113

¹ For practical purposes the values given in the table apply also to slabs the length of which with respect to the width is relatively great.

Stresses in a rectangular panel.—It remains to discuss the case of a rectangular panel. Let the edges have

the equations $x = \pm \frac{B}{2}$ and $y = \pm \frac{b}{2}$. Let $z = f(y)$ represent the solution for $B = \infty$ and b finite, and let $z = F(x)$ represent the analogous solution for B finite and $b = \infty$. Assume for the time being that Poisson's ratio is zero. Then, with the finite values of both B and b , the following solution will satisfy all the conditions:

$$z = f(y) + F(x). \quad (22)$$

With this solution the stresses σ_y may be found as if B were infinite, and the stresses σ_x as if b were infinite. It is a fact, however, that Poisson's ratio, μ , is not equal to zero. With $\mu=0.15$ the influence of this ratio is exemplified in Table 5, where the stresses σ_x vary from 90 to 107 pounds per square inch. If Poisson's ratio were zero, these stresses would all be 90 pounds per square inch. The variation is a matter of 18 per cent. If errors of this magnitude can be tolerated in a first approximation, then the solution indicated by equation 22 may be accepted as a first approximation. It may be noted that the radius of relative stiffness, l (see equation 11) is affected only slightly by a variation of Poisson's ratio, and the values of l given in Table 1, therefore, may still be used.

This consideration will be applied for the purpose of estimating the influence of curling due to a difference of temperature upon the corner break. The stresses due to the variation of temperature must be combined, in this case, with the stresses due to a wheel load acting close to the corner. Assume that the slab is 7 inches thick and that the resultant of a wheel load equal to 5,000 pounds is applied 4 inches from each of two edges which form the rectangular corner. Assume that the modulus of subgrade reaction is $k=100$ pounds per cubic inch. Then Table 1 gives $l=30.60$ inches. According to a previous paper¹⁰ the load produces in this case a tensile stress at the top equal to $\sigma_c = 0.5 \times 390 = 195$ pounds per square inch. This stress occurs in a section, which intersects the edges at a distance from the corner approximately equal to

$$x_1 \sqrt{2} = 2 \sqrt{2} \sqrt{4 \times 30.60} = 37.2 \text{ inches} = 0.860 l \sqrt{2}.$$

Both Figure 2 and Figure 3 indicate at this distance from the left of the diagram a temperature stress $\sigma = 0.40\sigma_c$. Figure 4 gives $\sigma = 0.34\sigma_c$. Since the maximum temperature stress occurs at a greater distance from the corner, one may obtain the maximum combined stress due to temperature and load by combining the stress due to load, $\sigma_c = 195$ pounds per square inch, with a temperature stress somewhat larger than $0.40\sigma_c$. The value $\sigma = 0.5\sigma_c$ may be considered to be a reasonable estimate. With $t=10$ degrees Fahrenheit, and the other numerical values as in the previous examples, except that $\mu=0$, one finds $\sigma_c = 90$ pounds per square inch, that is, $\sigma = 45$ pounds per square inch. Since the stress σ_c belongs in a section making an angle of 45 degrees with the edge, and the stress σ in a section perpendicular to the edge, the combined maximum stress will be, approximately, $\sigma_c + \frac{1}{2}\sigma = 195 + \frac{1}{2} \times 45 = 218$ pounds per square inch.

¹⁰ "Stresses in concrete pavements computed by theoretical analysis," Table 2, and equation 4.

ROAD PUBLICATIONS OF BUREAU OF PUBLIC ROADS

Applicants are urgently requested to ask only for those publications in which they are particularly interested. The Department can not undertake to supply complete sets nor to send free more than one copy of any publication to any one person. The editions of some of the publications are necessarily limited, and when the Department's free supply is exhausted and no funds are available for procuring additional copies, applicants are referred to the Superintendent of Documents, Government Printing Office, this city, who has them for sale at a nominal price, under the law of January 12, 1896. Those publications in this list, the Department supply of which is exhausted, can only be secured by purchase from the Superintendent of Documents, who is not authorized to furnish publications free

ANNUAL REPORTS

Report of the Chief of the Bureau of Public Roads, 1924.
Report of the Chief of the Bureau of Public Roads, 1925.

DEPARTMENT BULLETINS

- No. 105D. Progress Report of Experiments in Dust Prevention and Road Preservation, 1913.
- *136D. Highway Bonds. 20c.
- 220D. Road Models.
- 257D. Progress Report of Experiments in Dust Prevention and Road Preservation, 1914.
- *314D. Methods for the Examination of Bituminous Road Materials. 10c.
- *347D. Methods for the Determination of the Physical Properties of Road-Building Rock. 10c.
- *370D. The Results of Physical Tests of Road-Building Rock. 15c.
- 386D. Public Road Mileage and Revenues in the Middle Atlantic States, 1914.
- 387D. Public Road Mileage and Revenues in the Southern States, 1914.
- 388D. Public Road Mileage and Revenues in the New England States, 1914.
- 390D. Public Road Mileage and Revenues in the United States, 1914. A Summary.
- 407D. Progress Reports of Experiments in Dust Prevention and Road Preservation, 1915.
- *463D. Earth, Sand-Clay, and Gravel Roads. 15c.
- *532D. The Expansion and Contraction of Concrete and Concrete Roads. 10c.
- *537D. The Results of Physical Tests of Road-Building Rock in 1916, Including all Compression Tests. 5c.
- *583D. Reports on Experimental Convict Road Camp, Fulton County, Ga. 25c.
- *660D. Highway Cost Keeping. 10c.
- *670D. The Results of Physical Tests of Road-Building Rock in 1916 and 1917. 5c.
- *691D. Typical Specifications for Bituminous Road Materials. 10c.
- *724D. Drainage Methods and Foundations for County Roads. 20c.
- *1077D. Portland Cement Concrete Roads. 15c.
- *1132D. The Results of Physical Tests of Road-Building Rock from 1916 to 1921, Inclusive. 10c.
- *1216D. Tentative Standard Methods of Sampling and Testing Highway Materials, Adopted by the American Association of State Highway Officials and Approved by the Secretary of Agriculture for Use in Connection with Federal-Aid Road Construction. 15c.

- 1259D. Standard Specifications for Steel Highway Bridges adopted by the American Association of State Highway Officials and approved by the Secretary of Agriculture for use in connection with Federal-aid road work.
- 1279D. Rural Highway Mileage, Income, and Expenditures, 1921 and 1922.

DEPARTMENT CIRCULARS

- No. 94C. TNT as a Blasting Explosive.
- 331C. Standard Specifications for Corrugated Metal Pipe Culverts.

MISCELLANEOUS CIRCULARS

- No. 60M. Federal Legislation Providing for Federal Aid in Highway Construction.
- 62M. Standards Governing Plans, Specifications, Contract Forms, and Estimates for Federal-Aid Highway Projects.

FARMERS' BULLETINS

- No. *338F. Macadam Roads. 5c.
- *505F. Benefits of Improved Roads. 5c.

SEPARATE REPRINTS FROM THE YEARBOOK

- No. *739Y. Federal Aid to Highways, 1917. 5c.
- *849Y. Roads. 5c.
- 914Y. Highways and Highway Transportation.

REPRINTS FROM THE JOURNAL OF AGRICULTURAL RESEARCH

- Vol. 5, No. 17, D- 2. Effect of Controllable Variables upon the Penetration Test for Asphalts and Asphalt Cements.
- Vol. 5, No. 19, D- 3. Relation Between Properties of Hardness and Toughness of Road-Building Rock.
- Vol. 5, No. 24, D- 6. A New Penetration Needle for Use in Testing Bituminous Materials.
- Vol. 6, No. 6, D- 8. Tests of Three Large-Sized Reinforced-Concrete Slabs Under Concentrated Loading.
- Vol. 10, No. 5, D-12. Influence of Grading on the Value of Fine Aggregate Used in Portland Cement Concrete Road Construction.
- Vol. 11, No. 10, D-15. Tests of a Large-Sized Reinforced-Concrete Slab Subjected to Eccentric Concentrated Loads.

* Department supply exhausted.

UNITED STATES DEPARTMENT OF AGRICULTURE

BUREAU OF PUBLIC ROADS

STATUS OF FEDERAL AID HIGHWAY CONSTRUCTION

AS OF

APRIL 30, 1927

FISCAL YEAR 1927

STATES	FISCAL YEARS 1917-1926				PROJECTS COMPLETED SINCE JUNE 30, 1926				*PROJECTS UNDER CONSTRUCTION				PROJECTS APPROVED FOR CONSTRUCTION				BALANCE OF FEDERAL AID FUND AVAILABLE FOR NEW PROJECTS		STATES
	PROJECTS COMPLETED PRIOR TO JULY 1, 1926				TOTAL COST				ESTIMATED COST				ESTIMATED COST				FEDERAL AID ALLOTTED		
	TOTAL COST	FEDERAL AID	MILES		TOTAL COST	FEDERAL AID	MILES		ESTIMATED COST	FEDERAL AID ALLOTTED	MILES		ESTIMATED COST	FEDERAL AID ALLOTTED	MILES				
Alabama	18,226,411.34	8,725,985.09	1293.3		1,834,980.24	889,114.85	101.9		6,566,145.16	3,127,211.59	381.3		250,531.48	136,675.57	14.3		3,017,687.90	Alabama	
Arizona	10,949,678.25	5,653,772.35	729.8		741,370.79	508,759.34	48.6		1,166,448.59	791,184.87	73.0		244,878.65	176,216.27	11.7		3,334,270.17	Arizona	
Arkansas	18,364,544.50	7,668,698.35	1323.0		3,825,393.39	1,768,703.69	227.7		2,446,897.77	1,179,389.37	189.5		1,004,351.69	501,815.84	39.3		1,747,092.75	Arkansas	
California	27,142,596.90	13,003,582.30	1058.0		7,751,763.63	3,834,300.45	240.6		7,355,382.51	3,419,674.51	152.9		89,175.17	37,146.93	2.1		4,261,537.81	California	
Colorado	13,805,904.64	7,187,288.18	745.0		1,500,384.22	758,603.83	72.4		6,348,324.16	3,075,282.41	278.5		168,779.97	104,700.27	12.1		2,636,397.31	Colorado	
Connecticut	4,414,587.19	2,100,585.80	117.1		694,812.28	245,719.74	13.7		5,693,320.98	1,575,579.68	70.4		189,263.32	94,641.66	0.3		789,838.92	Connecticut	
Delaware	4,918,052.29	1,781,665.60	124.3		1,039,483.07	425,057.18	28.0		831,815.88	361,826.46	31.7		271,652.15	63,316.77	6.4		180,807.05	Delaware	
Florida	3,632,680.26	1,824,362.32	132.9		3,644,176.05	1,803,950.28	112.1		9,676,945.85	3,777,276.07	166.3		1,190,401.52	217,353.96	8.3		1,181,124.55	Florida	
Georgia	24,791,206.97	11,664,237.66	1794.0		5,985,294.06	2,712,309.78	307.6		9,251,767.30	4,546,622.72	398.3		4,62,600.34	217,353.96	8.3		1,270,668.08	Georgia	
Idaho	11,061,198.14	5,682,112.70	724.7		2,164,317.31	1,193,414.46	110.8		2,109,090.97	1,324,331.38	162.2		682,439.37	403,115.31	40.1		691,846.15	Idaho	
Illinois	44,111,611.86	20,619,995.74	1377.7		4,206,434.39	2,055,293.14	143.4		6,476,356.55	4,039,284.18	304.4		6,069,197.47	3,034,099.60	211.5		3,237,954.34	Illinois	
Indiana	16,945,425.87	8,172,125.19	534.3		4,816,445.63	2,217,149.61	153.8		16,282,739.48	7,642,949.67	482.3		2,655,991.68	1,324,331.38	97.2		775,957.20	Indiana	
Iowa	29,062,375.40	11,926,302.10	2114.8		4,811,414.00	2,254,019.86	331.0		11,897,891.73	5,346,201.12	536.9		4,471,438.94	1,814,732.08	110.5		189,306.94	Iowa	
Kansas	32,826,301.64	12,580,469.25	1160.6		3,941,604.35	1,847,691.55	282.3		12,948,000.44	5,122,199.09	649.5		1,998,000.33	751,823.22	18.8		1,650,151.16	Kansas	
Kentucky	20,757,706.10	6,492,082.25	786.3		2,243,696.75	915,931.55	100.1		9,235,987.23	4,356,476.31	413.2		1,582,422.54	365,473.56	48.3		3,011,330.33	Kentucky	
Louisiana	13,830,982.68	6,144,739.99	1056.9		1,911,816.79	881,581.86	111.0		4,234,632.21	1,993,413.53	149.7		26,200.66	13,100.33	3.0		1,282,880.29	Louisiana	
Maine	8,747,582.75	4,182,507.39	303.6		1,817,247.30	865,945.28	54.0		2,231,036.53	621,344.43	63.4		67,912.01	43,196.00	5.6		1,445,635.00	Maine	
Maryland	10,324,937.10	5,112,251.22	353.3		1,863,260.83	1,114,947.05	53.3		8,914,475.47	3,712,185.94	33.3		887,123.10	193,770.00	12.9		2,374,833.28	Maryland	
Massachusetts	16,324,937.71	8,167,260.92	374.5		1,789,185.97	604,492.53	24.9		13,124,680.48	1,307,469.87	33.2		1,695,050.00	780,700.00	40.6		2,403,429.19	Massachusetts	
Michigan	23,297,240.71	11,657,260.92	948.0		3,941,604.35	1,847,691.55	282.3		1,549,479.24	1,333,488.24	122.2		2,100,527.65	695,737.23	145.5		5,659,689.84	Michigan	
Minnesota	37,170,985.95	15,566,116.56	3181.8		7,528,682.52	3,460,029.11	481.6		4,398,005.64	1,306,198.90	268.0		2,985,440.85	789,700.00	119.2		560,476.43	Minnesota	
Mississippi	15,146,089.52	7,414,534.10	1120.0		2,250,931.37	1,145,635.10	138.0		6,921,252.88	3,370,848.33	372.0		1,186,162.97	575,034.21	65.2		928,846.26	Mississippi	
Missouri	23,989,165.92	11,736,014.85	1543.2		1,276,539.34	4,777,832.80	32.0		10,705,719.54	3,370,848.33	372.0		1,754,125.97	751,595.43	84.3		1,366,401.01	Missouri	
Montana	11,407,983.81	6,333,465.89	1054.9		1,454,011.91	953,832.80	96.7		1,549,479.24	1,333,488.24	122.2		2,100,527.65	695,737.23	145.5		5,659,689.84	Montana	
Nebraska	11,533,401.62	5,474,202.52	1768.3		4,243,144.09	2,085,953.55	428.2		10,863,610.88	5,404,351.04	1167.8		2,422,195.43	1,194,381.26	176.5		2,060,944.53	Nebraska	
Nevada	7,559,195.51	5,130,934.59	538.8		2,731,485.04	2,351,683.67	300.4		1,639,091.95	1,418,223.54	197.1		1,717,771.61	1,194,381.26	176.5		842,883.20	Nevada	
New Hampshire	4,992,558.60	2,377,450.07	237.6		846,458.09	386,537.45	25.4		647,214.00	303,892.51	18.7		201,149.13	95,178.55	7.4		372,148.42	New Hampshire	
New Jersey	16,346,301.01	5,098,342.21	290.3		5,891,939.07	2,397,022.87	26.0		4,726,000.24	970,846.60	59.8		2,346,992.79	598,976.96	42.8		335,842.96	New Jersey	
New Mexico	12,404,337.77	7,339,657.38	1427.0		826,132.76	501,532.01	71.4		3,443,308.01	2,684,953.75	240.6		7,917,333.00	1,762,327.50	98.9		1,633,005.86	New Mexico	
New York	43,224,279.79	17,311,957.19	1197.0		9,680,900.60	3,355,217.96	216.8		35,451,253.00	9,060,878.95	565.2		7,917,333.00	1,762,327.50	98.9		5,589,430.40	New York	
North Carolina	27,009,419.47	11,177,337.94	1257.9		7,799,414.95	3,135,240.32	189.3		2,673,142.76	1,267,391.42	79.3		1,169,231.30	517,189.76	34.3		1,333,412.57	North Carolina	
North Dakota	12,313,311.40	6,031,859.78	2153.1		3,850,008.60	1,708,423.60	582.3		4,392,396.06	2,426,054.74	642.5		2,113,129.30	1,056,417.74	264.8		720,844.14	North Dakota	
Ohio	47,599,532.90	17,317,787.03	1364.1		4,921,858.59	1,959,589.73	150.9		11,323,622.56	4,369,902.25	323.8		633,896.16	219,093.22	12.8		4,553,632.77	Ohio	
Oklahoma	28,247,950.33	13,159,999.15	1178.9		1,886,210.72	858,132.39	73.8		3,259,630.69	1,366,982.43	203.9		1,977,435.69	692,603.25	119.1		1,527,980.78	Oklahoma	
Oregon	17,027,878.42	8,593,214.79	939.2		1,937,591.20	1,156,191.52	97.1		2,627,483.66	1,402,557.40	66.4		3,978,264.56	1,458,563.64	83.3		709,878.94	Oregon	
Pennsylvania	61,366,150.80	21,560,732.04	1188.8		14,254,516.22	4,139,471.13	303.9		15,315,924.81	4,483,337.98	304.5		3,978,264.56	1,458,563.64	83.3		3,031,605.01	Pennsylvania	
Rhode Island	3,988,616.08	1,588,829.06	86.7		1,244,797.29	439,650.00	29.3		778,986.12	205,665.00	13.7		957,110.35	237,810.00	15.8		591,239.94	Rhode Island	
South Carolina	15,020,639.90	6,766,322.93	1481.9		1,981,400.03	760,665.87	86.5		6,163,986.71	2,575,506.55	206.2		261,249.54	108,116.82	21.4		645,897.83	South Carolina	
South Dakota	17,468,373.19	8,603,826.97	2181.2		3,901,199.30	668,439.27	62.5		2,198,402.66	1,672,855.84	161.8		1,694,196.26	813,238.16	69.7		903,306.33	South Dakota	
Tennessee	21,624,631.57	10,276,584.02	780.0		2,562,789.67	1,229,742.90	78.8		8,316,331.91	3,468,402.56	235.6		111,887.73	35,000.00	0.3		1,885,627.52	Tennessee	
Texas	69,183,673.48	27,440,254.72	4920.2		8,371,957.91	3,821,639.25	531.8		15,391,788.95	6,831,159.89	527.5		1,694,196.26	813,238.16	69.7		6,197,557.28	Texas	
Utah	8,253,178.03	5,098,440.68	946.4		901,199.30	668,439.27	62.5		2,198,402.66	1,672,855.84	161.8		1,694,196.26	813,238.16	69.7		1,142,630.52	Utah	
Vermont	4,242,042.64	2,017,699.51	134.5		754,443.45	315,571.50	17.2		1,501,129.86	564,170.08	23.9		1,071,311.26	422,028.44	26.9		314,682.47	Vermont	
Virginia	21,990,249.44	10,365,726.11	1005.5		4,562,420.13	1,957,920.17	149.7		4,846,810.87	1,966,510.87	113.1		1,071,311.26	393,530.29	21.9		180,480.46	Virginia	
Washington	17,078,511.63	7,782,905.46	898.2		1,105,934.34	432,642.49	42.5		3,690,400.86	1,750,800.00	82.2		273,990.33	50,501.38	10.2		1,229,554.67	Washington	
West Virginia	9,473,716.44	4,141,082.65	782.9		551,130.88	432,642.49	26.5		7,132,862.00	2,934,191.85	238.2		109,976.65	54,584.32	5.7		585,216.02	West Virginia	
Wisconsin	24,856,508.19	10,392,705.73	1592.1		2,758,432.85	1,324,002.42	124.1		6,902,373.50	3,283,441.30	301.6		3,068,668.14	1,378,265.50	86.9		2,929,850.05	Wisconsin	
Wyoming	10,928,302.98	6,040,187.05	1133.5		1,722,409.59	1,098,300.00	102.4		1,695,770.51	1,025,887.63	104.2		285,445.77	222,920.28	34.5		1,112,768.04	Wyoming	
Hawaii	805,375.36	343,664.15	6.5		1,786,323.89	562,462.84	29.7		1,786,323.89	562,462.84	29.7		64,117,127.86	25,443,083.76	2,531.7		805,375.36	Hawaii	
TOTALS	365,652,834.16	182,653,192.83	12,526.8		168,653,192.83	75,541,420.87	7,701.2		318,656,492.63	134,459,557.35	1								

* Includes projects reported completed (final vouchers not yet paid) totaling: Estimated cost \$ 71,805,434.08 Federal aid \$ 30,995,665.91 Miles 2,721.6